ECN

Energy research Centre of the Netherlands

Model Experiments in Controlled Conditions

Final Report

J.G. Schepers

H. Snel

ECN-E--07-042

Acknowledgement/Preface

Financial support for this research was given in part by the European Commission's Fifth Framework Programme. Project Reference: ENK5-CT-2000-00309, Mexico: Model rotor EXperiments In COntrolled conditions. Furthermore the Dutch contribution in the project was partly financed by SenterNovem, an agency of the Dutch Ministry of Economic Affairs, under the TWIN programme. The contract number was 0224-01-57-21-0013 (ECN project 7.4121).

Abstract

Within the framework of the EU FP5 project MEXICO, a sophisticated aerodynamic experiment was designed, and executed in the LLF (Large Scale Low Speed Facility) of the German Dutch Wind tunnel Organisation (DNW). A three bladed rotor model of 4.5 m diameter was designed and manufactured, including a speed controller and pitch actuator. The model was instrumented with 148 Kulite® pressure sensors, distributed over 5 sections of the blades; strain gauges bridges were applied to the three blade roots for the registration of bending moments in two directions. The model was mounted on the wind tunnel 6 components balance, were total forces and moments were measured. Finally a large number of Particle Image Velocimetry (PIV) studies were programmed, to determine the flow field around the rotor, the inflow and near wake, and to track tip vortices.
The experiment was designed fort the 9.5*9.5 m^2 open test section of the LLF. Detailed studies were executed to enable tunnel corrections on the measurements.
The measurement programme was executed in December of 2006. All planned measurement data was obtained, and forms a 100 GB database of detailed aerodynamic information, available to all consortium members. Initial data processing has been performed which will lead to improvements of design methods and to validate CFD methods.

FINAL REPORT

CONTRACT N° : ENK5-CT-2000-00309

PROJECT N° : ENK5-CT-2000-00309

ACRONYM : MEXICO

TITLE : Model Experiments in Controlled Conditions

PROJECT CO-ORDINATOR : The Energy Research Center of the Netherlands ECN

PARTNERS :

- National Aerospace Laboratory NLR (NL)
- Delft University of Technology DUT (NL)
- Israel Institute of Technology TECHNION (IL)
- Risoe National Laboratory (DK)
- Danish Technical University DTU (DK)
- Swedish Defence Research Agency FOI (SE)
- Centre for Renewable Energy Sources CRES (GR)
- National Technical University of Athens NTUA (Associate) (GR)

PROJECT START DATE : 1/1/2001 DURATION : 72 months

Date of issue of this report : February 2007

Project funded by the European Community under the '5th Framework' Programme (1998-2002)

TABLE OF CONTENTS

1. EXECUTIVE SUMMARY 3
1.1 OBJECTIVES 3
1.2 WORK PERFORMED 3
1.3 RESULTS 8

2. DETAILED FINAL REPORT
2.1 OBJECTIVES AND STRATEGIC ASPECTS 11
2.2 SCIENTIFIC AND TECHNICAL DESCRIPTION OF THE RESULTS 12
2.2.1 Introduction 12
2.2.2 Activities and results of Phase 1 (design and tunnel effects) 13
2.2.3 Activities and results of Phase 2 (preparation of the measurement and the data acquisition) 16
2.2.4 Activities and results of Phase 3 (Measurements) 21
2.2.5 Activities and results of Phase 4 (Analysis of measurements) 23

2.3 ASSESSMENT OF RESULTS AND CONCLUSIONS 26
2.4 ACKNOWLEDGEMENT 29
2.5 REFERENCES 29

3. MANAGEMENT FINAL REPORT
3.1. LIST OF DELIVERABLES 31
3.2 COMPARISON OF INITIALLY PLANNED ACTIVITIES AND WORK ACTUALLY ACCOMPLISHED 32
3.3 MANAGEMENT AND CO-ORDINATION ASPECTS 33

1. EXECUTIVE PUBLISHABLE SUMMARY

1.1 Objectives

With the growing size and investment cost of wind turbines, there is an equally growing demand for more reliable design methods. This is especially the case for offshore turbines, where the reliability of the machine and its design are among the most important challenges. At present the uncertainty in design calculations is 10%-20% for performance prediction and 30% for dynamic load prediction.

The principal objective of this project is to significantly reduce these uncertainties by providing an experimental database, measured in a large wind tunnel under controlled and hence known conditions and by using the increased physical insight resulting from the experiments in engineering design methods. At the same time, the database is necessary to provide a validation tool for the upcoming area of Navier Stokes based calculation techniques. The improvement of engineering design codes is a short-term objective; it will be available shortly after the end of the project. The effect of Navier Stokes validation on the design practice can be expected to take place within a period of five to seven years.

In order to meet these objectives, the project was carried out in four phases. The first phase culminated in the detailed design of a sophisticated wind tunnel model to be tested in the Large Scale Low Speed (LLF) facility of the DNW. The second phase consisted in the construction and instrumentation of the model, the design and manufacturing of the data transfer and data acquisition system and the design of the experiment, i.e. the detailed programme of measurements and conditions to be covered. The actual performance of the measurement campaigns, the data processing and the data interpretation was done in the third phase. Finally the fourth phase consisted in a limited number of comparisons from BEM and Navier Stokes models with measured data. Moreover, the available data are organized in a data base for better access.

1.2 Work performed

The most important activity in the project was obviously Phase III (i.e. the performance of the experiment in the wind tunnel). This experiment was carried out in the period from December 6th to December 14th 2007.
The experiment (in terms of wind tunnel, turbine model, instrumentation, measurement techniques and test matrix) can be characterised in the following way, where an overall view of the experimental set-up and the wind tunnel is given in the figures 1.1 and 1.2.

Figure 1.1: Turbine model mounted on balance in open test section

Figure 1.2: LLF wind tunnel of DNW

- Wind tunnel: The LLF wind tunnel of the German Dutch Wind Tunnel Facilities (DNW) was used with an open test section of 9.5 x 9.5 m^2, where flow is blowing from a nozzle to a collector (with a closed loop between collector and nozzle). The wind tunnel is located in the North East Polder in the Netherlands;
- Model rotor:
  - Number of blades: Three
  - Diameter: 4.5 m (i.e. blade radius = 2.25 m)
  - Rotational direction: clockwise when looking to the rotor
- Control

- Fast electrical speed control. It is noted that the rotor speed was usually kept constant at 424.5 rpm (~ 7Hz). A limited number of measurements at 324.5 rpm and standstill have also been performed.
- Fast pitch control

- Tower: The tower was mounted on a yawable DNW-balance for the measurement of 3 forces and 3 moments at the bottom of the tower.
- Blades:
  - Airfoils families:
    - DU 91-W2-250 at the root of the blade;
    - RISØ A1-21 at mid span;
    - NACA 64-418 at the outer part of the blade.

    The 2D aerodynamic characteristics of these airfoils were also measured as a reference to the rotating measurements.
  - The blades were twisted and tapered.
  - A zig-zag tape was applied at 5% of the chord (both at the pressure and suction side) to provoke transition and to avoid laminar separation.
- Pressure measurements: The blades were instrumented with 148 fast Kulite pressure sensors to measure the pressure distribution around the airfoils in terms of absolute pressures. The pressure transducers were mounted at 25%, 35%, 60% 82% and 95% span, where the number of pressure transducers per station varied between 25 to 28. The pressure transducers were connected to PCB's (Printed Circuit Boards) in the blade from which the data were led (digitally) over a slip-ring to the data acquisition units in the non-rotating part of the model. In view of conflicting requirements between structural needs on one hand, and the required space for the PCB's in the model blade on the other hand, it was not possible to mount all pressure sensors into 1 blade. For this reason they were divided over all three blades (where blade 1 has the instrumented sections at 25% and 35% span, blade 2 is instrumented at 60% span and blade 3 is instrumented at 82 and 95%). A limited number of pressure sensors were mounted at similar locations at the other blades to check the reproducibility of the pressure measurements on the different blades
- Blade root bending moments: The blades have been instrumented with strain gauges at the root of all three blades to measure the root bending moments. Furthermore a temperature sensor has been mounted in 1 of the blades.
- 1P trigger sensor. An optical 1P sensor was mounted which generated a trigger signal when blade 1 was passing the 12 o'clock position. This position is defined to be the zero azimuth angle.
- PIV measurements: The PIV (Particle Image Velocimetry) technique made it possible to determine the 3D flow field in a detailed quantitative way, both upstream and downstream of the model. The PIV measurements were performed in the following way:
  - A PIV traversing tower with two camera's focussed on a PIV sheet (337*394 mm) in which the flow field is measured. The PIV sheet is located horizontally in the symmetry plane of the rotor at the 270 degrees azimuth position (i.e. at the 9 o' clock position).
  - The PIV tower was mounted on a traversing mechanism, which made it possible to traverse PIV sheets in a horizontal plane where the range in axial direction is approximately 10 meters and the range in radial direction is approximately 1.2 m (see below).
  - Seeding (in the form of small bubbles) was introduced in the settling chamber, upstream of rotor.

- The seeded PIV sheet is illuminated with a strong laser flash, and two digital photographs are taken with a delay of only 200 nanoseconds and a comparison is made between the two 'seeding fields';
- The PIV sheet is then subdivided into small ‘interrogation windows’ and a large number of velocity vector fields are 'attempted'. The actual velocity vector is the one resulting in maximum cross correlation between the two 'seeding fields'

o Definitions: The definitions and conventions to be used in the experiment were harmonised. For the interpretation of data, the definition of azimuth angle, blade numbering and yaw angle is of particular importance:
  - o Definition of azimuth angle: The zero azimuth position is defined to be the 12 o'clock position for blade number 1 (i.e. the position where the trigger signal is given).
  - o Blade numbering: The order in which the blades pass the tower is: 1,2,3
  - o Definition of yaw angle, see figure 1.3

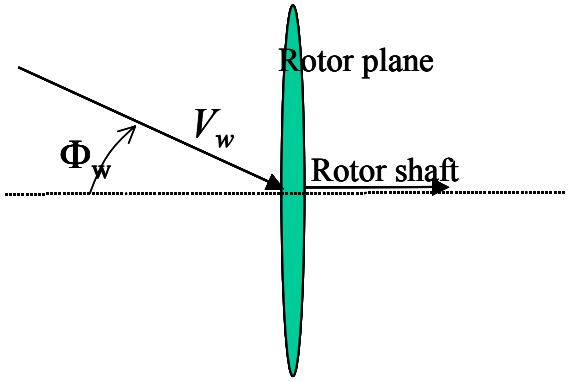

Figure 1.3: Definition of yaw angle (ϕ_w)

o Data points, sampling frequency and measurement period:
  - The first data points were taken without the PIV measurements, hence these data points only include the measurement of the pressure distributions and the blade root bending moments in conjunction with the measurement of the tunnel data (tunnel speed etc). In the sequel these data points are denoted as 'pressure data points'. The later data points included the PIV measurements where the blade and tunnel data were measured simultaneously. These data points are denoted as 'PIV data points'.
  - Pressure data points:
    A pressure data point is defined as a recording during which the conditions (in terms of tunnel conditions and model configuration) remained constant (the only exception lies in the dynamic inflow measurements, see below, where a data point includes a step in pitch angle or rotor speed). The pressure and blade root bending moments are sampled with a frequency of 5.5 kHz (effectively 1.5 kHz). In most cases the rotor speed was approximately 7 Hz. This implies that the measurements were taken at every 1.7 degrees angular interval. The measurement period was 5 seconds (i.e. 35 revolutions for a rotor speed of 7 Hz).
  - PIV data points. A PIV data point is defined as the measurement of a flow vector field within a PIV sheet during which the conditions in terms of tunnel

conditions and model configuration remained constants. A data point is composed of 100 'frames' where a 'frame' is the result of the two subsequent photographs (see above). The frames are all made at a given blade position ('Phase locked'). The sampling frequency between two frames is approximately 2.4 Hz, which enabled a 'phase locked' measurement (note that the rotor speed was 7.075 Hz). The resulting measurement period for a PIV data point in then in the order of 40 seconds.

- Tunnel and balance data: The tunnel data (tunnel speed, pressure, temperature) and the balance data were averaged over a data point.

o Test matrix. A total of 50 hours of tunnel time (including the installation and the dismantling of the model) had been subcontracted to DNW. Within this period 944 data points could be taken:

- Pressure data points: The first 257 data points were taken without the PIV recordings. These measurements were done for the following conditions:
  - Axisymmetric conditions
    - Rotor speed: 324.5 rpm and 424.5 rpm (V_{tip} = 76 and 100 m/s or 5.35 Hz and 7 Hz)
    - Tunnel speed: Between 5.5 to 30 m/s
    - Pitch angles: Between -5.3 and 1.7 degrees
  - Yawed conditions: Measurements have been performed at yaw angles of 15, 30 and 45 degrees and tunnel speeds of 10, 15, 18 and 24 m/s. The pitch angle = -2.3 degrees
  - Dynamic Inflow: Fast pitching steps and rotor speed steps have been measured at tunnels speeds of 10, 15, 18 and 24 m/s. It must be noted that the pitch angle was not measured directly but the begin and end values were recorded. The pitch angle varied between -2.3 and +5 degees. This pitching step was supposed to take place within 0.05 seconds. The rotor speed was derived from the 1P trigger sensor.
  - Parked rotor measurements. Parked rotor measurements have been done at a tunnel speed of 30 m/s and pitch angles ranging between -2.3 and 90 degrees
- PIV data points (Note that the PIV measurements were combined with measurements of the pressures and the blade root moments). Approximately 700 PIV datapoints have been taken at the following conditions:
  - Axi-symmetric conditions at a tunnel speed = 10, 15 and 24 m/s, a rotor speed of 424.5 rpm and a pitch angle = -2.3 degrees Furthermore measurements have been performed at pitch angles of -5.3 and 0.7 degrees and a tunnel speed of 24 m/s. The following traverses have been made:
    - Two radial PIV traverses from r = 1.374 m to r = 2.54 m (i.e. from r/R = 0.61 to r/R = 1.29) at x = -0.15 and x = 0.15 m (i.e. at x = 0.066 R upstream and downstream of the rotor plane). It is noted that these locations refer to the PIV sheet centers. The radial traverses are performed at 6 blade azimuth positions with a 20 degrees azimuth interval (where the 3P flow dependency makes it sufficient to cover only 120 degrees azimuth).
      It is noted that these radial traverses are <u>not</u> made for pitch angles of -5.3 and 0.7 degrees.
    - Two axial traverses from x = -4.325 m to x = 5.725 (i.e. from 1.92 R upstream of the rotor to 2.54 R downstream of the rotor

at r = 1.374 m and y = 1.845 m (i.e. at r/R = 0.61 and r/R = 0.82). The locations again refer to the centres of the PIV sheet. The traverses are made for 1 blade azimuth position (in most cases the measurements were done for zero azimuth of blade 1);

- Vortex search: For a given blade azimuth angle (usually 270 degrees azimuth of blade 3), the position of the tip vortex is searched by 'trial and error' at a large number of axial positions.

- Yawed conditions: Yawed measurements have been performed at yaw angles of plus and minus 30 degrees and a tunnel speed of 15 m/s, where the pitch angle = -2.3 degrees. Both axial and radial traverses have been performed in a procedure very comparable to the procedure as described at aligned conditions. The locations of the PIV sheets were also more or less similar. Furthermore a vortex search has been carried out.
  In view of the fact that the PIV sheets were located in the horizontal symmetry plane at an azimuth angle of 270 degrees, the measurements at the plus and minus yaw angle represent the flow field at two opposite azimuth angles (90 and 270 degrees) for the same yaw angle.

1.3 Results

The most important results from the project are:

- An extensively instrumented wind turbine model. This model can be used for future wind tunnel experiments and/or field experiments.
- A database of unique detailed aerodynamic measurements on a representative wind turbine model taken in the largest wind tunnel of the EU. The data (100 Gbytes) are organised in a self explanatory way on external hard discs and distributed between the participants. On the disc, the time series (of pressures and strain gauges) are given in raw form. Furthermore some processed data are stored in ASCII format. The disc also contains a data point overview and the basic software with which the raw time series can be processed. The PIV data are given in processed form (i.e. ASCII data of the velocity vectors at different x-y-z positions).
- In view of the fact that the measurements have been taken from December 6 until December 14, 2007 where the end date of the project was December 31, 2007, only very little time was left for analysis of data. Nevertheless quality assessment of the data could be performed and some first very important new insights on the flow field around the rotor have already been gained. In the near future these new insights will definitely help to validate and improve aerodynamic wind turbine models:
  - The PIV traverses in axial direction allowed, for the first time ever, a detailed appraisal of the development of the induction upstream and downstream of the rotor. This is important information for BEM codes, CFD codes and free wake models. A comparison between the measured slow down of the velocities in the wake and a theoretical estimate shows a very good agreement at 82% span but a poor agreement at 61% span which is due to the release of strong trailing vorticity near that location. At higher thrust coefficients, clear indications have been found for increased turbulent activity, which is most likely related to the turbulent wake situation.
  - Some very unique details of the tip vortex could be made visible. The measurement of the v-component formed a perfect basis for such study and enabled the determination of the vortex core diameter and the maximum

rotational speed in the wake of a wind turbine. This definitely will help to improve free vortex wake models.

- The bound vortex strength has been estimated using the measurements of the pressure distributions along the blade. The estimated value compares very well with the tip vortex strength measured with PIV. This is again very important information for free vortex wake models.
- The tip vortex trajectories could be determined. A clear expansion is found which is largest for the lower tunnel speeds. The resulting transport velocities of the tip vortices do not seem to decrease with downstream distance. This is contrary to some intuitive models, which assume that the transport velocity is the average of the wake speed and the undisturbed outer speed.
- For the first time ever, it has been possible to measure the induction between the blades. Towards the tip, these measurements can be used to refine tip correction models, even for yawed flow.
- For the first time ever, the velocity field from the viscous wake which is released from a rotor blade has been measured. This is important information for all types of wind turbine codes.
- The pressure distributions at 60% span and a tunnel speed of 24 m/s show the expected behaviour: At aligned flow, they indicate an axi-symmetric flow (i.e hardly any azimuthal variation in pressure distributions is found) and they indicate a stalled boundary layer, as expected at this high tunnel speed. At yawed flow, the pressure distributions show a cyclic stalled/unstalled variation.
- The response of the normal force to the rotor speed ramp does show an overshoot.
- A preliminary c_n-α curve has been derived at parked conditions, which at least for some sections, compares reasonably well with the expected 2D airfoil characteristics.
- With regard to the quality of the data the following preliminary conclusions were drawn:
    - The PIV measurement give a very detailed and consistent picture of the flow field, in terms of induction, vortex transport velocities, vortex structures and even the velocity field from the viscous wake of the rotor blade could be measured. The analyses, which have been performed were a testimony to the great flow detail present in the PIV measurements.
    - Generally speaking, the pressure distributions at 60, 82 and 92% span look reliable. This is confirmed by a good to reasonable agreement between the pressures at the different blades (and similar positions). The good quality is also confirmed by a good repeatibility of the data. Repetition runs indicated hardly any change in pressure distributions, even after 1 week. The pressure distributions at 25% and 35% do not always comply with the expectations. It is suspected that this is due to a slight instable behaviour of the Kulite pressure transducers in combination with very low pressures at the inner part of the blade. It is then important to note that frequent zero runs have been carried out due to zero drift, but this drift could be a substantial fraction of the pressures at the inner part of the blade.
    - The response of the normal force to the pitching ramp leads to the suspicion that the ramp is somewhat slower than specified.
    - The blade root bending moments seem reliable on two blades. The (less

relevant) moments on the third blade look less reliable which is due to outliers in the calibration.

- The balance data give a consistent picture of the loading at the tower foot although it is suspected that a few loads are in the lower end of the measurement range.

Altogether it is expected that the resulting database will serve the wind community for many years to come as a basis for further model improvement and validation.

2 DETAILED FINAL REPORT

2.1 Objectives and strategic aspects

Several studies, among which the EU study VEWDTC [2] have indicated that the main contributions to the uncertainty in the loads of a wind turbines result from the aerodynamic modelling in the computer programmes used for load calculations. These uncertainties may to a certain degree translate into the use of high safety factors in the certification processes, but certainly do form a main cause for design risks. This becomes a major problem with the growing size and investment cost of wind turbines, both for on-land and for offshore use.

It is of strategic importance for the wind turbine industry to reduce the uncertainties and risks and the present project addressed this problem through thorough aerodynamic measurements under controlled conditions, in the largest wind tunnel of the EU. The measurements will lead to improved insight and knowledge, for all operational conditions, including stall and yawed inflow conditions, which eventually will be implemented in design tools. Recently, such a measurement programme was executed in the NASA-Ames wind tunnel by the National Renewable Energy Laboratories of the USA. The experiments performed in the present project were designed to be complementary with the NREL measurements (e.g. a three-bladed rotor will be used as compared to the two-bladed NREL rotor) to further enhance the value, and to negotiate the exchange of data with NREL. Another crucial difference is the fact that in the present project the flow field in the rotor plane has been measured simultaneously with the blade flow properties. (The NREL measurements are restricted to blade loads and blade pressure distributions.)

Since the prospect of improved aerodynamic modelling as a result of the present project will definitely strengthen Europe's design capabilities, the project in this sense is crucial in maintaining Europe's leading position in the design and construction of large wind turbines.

The participants, in executing this pivotal project, will enhance their market position in wind energy design support. Although eventually most results will become available to the entire wind energy community, first knowledge derived from active participation in the project will definitely represent an advantage.
For the future, the project opens the door for a further use of high-level computational tools such as Euler codes (e.g. free vortex wakes) and Navier-Stokes solvers by providing the first useful database of measured and high-quality flow field results. Within the further development of Navier-Stokes codes, transition and turbulence modelling are essential, particularly but not exclusively regarding the influence on stalled flows. The database from the present project will be the only one of sufficient detail and accuracy to provide validation for these models, under a wide variety of flow conditions.

It is also quite likely that the observations and measurements will lead to new physical insights. In the other case, the final results will lead to a confirmation of present insight, and contribute to further development of existing and new aero-elastic simulation codes for wind turbine design.

2.2 Scientific and Technical description of the results.

2.2.1 Introduction

In this chapter the different Phases and Work Packages of the project are described. The work plan consisted of four phases, which are further subdivided in different Work Packages. The first phase culminated in the detailed design of a sophisticated wind tunnel model to be tested in the Large Scale Low Speed (LLF) facility of the German Dutch Wind tunnel, DNW which is located in the North East Polder in the Netherlands. The second phase consisted in the construction and instrumentation of the model, the design and manufacturing of the data transfer and data acquisition system and the design of the experiment, i.e. the detailed programme of measurements and conditions to be covered. The actual performance of the measurement campaigns and the data processing was done in the third phase. Finally the fourth phase consisted in a limited number of initial comparisons from BEM and Navier Stokes models with measured data. Furthermore the available data are organized in a base for easy access.

The project started on January 1, 2001 and it was originally scheduled to end on December 31, 2003. The project got off to a difficult start because of the bankruptcy of Aerpac, one of the contractors, in January 2001. This caused a hold on the side of the EC, including the decision not to disburse the advance payment, until a replacement contractor was found and accepted by the EC in the form of the blade manufacturer Polymarin B.V. Unfortunately Polymarin B.V. went bankrupt in November 2002, causing another difficult period in the project. After a long period of negotiations the PCC (i.e. the Project Steering Committee) preferred a continuation of the project without a replacement of Polymarin where Polymarin's tasks were taken over by other participants.

Moreover the project suffered from some technical delays and it underwent some changes, which resulted in an adjusted planning. In view of the fact that the possibilities of a new measurement technique, i.e. the Particle Image Velocimetry (PIV) technique became very promising, it was decided to apply this technique in the Mexico project. This decision was believed to be (and turned out to be!) very positive for the quality of the results. Thereto it should be realised that the original plan was to measure the flow field downstream of the rotor with a so-called wake rig. This however would definitely have become a very delicate instrument, which would only have provided low resolution data in a very intrusive way. Another delay was caused by calculations on wind tunnel effects which indicated that these could be much more severe than originally expected. Although dedicated numerical and analytical analysis led to the understanding and modelling of corrections for the effect it was nevertheless decided to perform an additional wind tunnel test in a so-called pilot tunnel of the large DNW-LLF tunnel, see [17].

At the same time, more time appeared necessary to solve problems in the design of the wind tunnel model and the Data Acquisition Hardware. Conflicting requirements appeared between structural needs on one hand and the required space for the electronics in the model blade on the other hand. The original decision to mount all pressure sensors in one blade even had to be reconsidered. It was also decided to use the DNW tunnel balance for the measurement of the integral rotor loads. Mounting this balance was very time consuming and was charged from the available tunnel time. Hence the available tunnel time for the actual tests was reduced and led to the decision to perform all measurements within 1 tunnel slot where originally two tunnel slots were planned. Another important delay was caused by an accident, which

happened in January 2005 during transportation of the wind turbine model to the DNW-LLF wind tunnel in the Netherlands. The model suffered from severe damage and the necessary repairs were very time consuming and costly.

As a result of these delays, the original scheduled end time of December 31st 2003 was no longer realistic. The final end data eventually moved to December 31st 2006. It should then be realised that the tunnel measurements were executed in December 2006, which obviously left very little time for analysis of the data.

The minutes of all plenary meetings and of the task group meetings can be found on the MEXICO web page, on the ECN 'extranet' site, accessible via password protection. On this site, also task reports can be found.

An important activity was the harmonisation of definitions and conventions to be used during the wind tunnel test. Most important for the interpretation of data, is the definition of azimuth angle, blade numbering and yaw angle. The following definitions have been applied:

- Definition of azimuth angle: The zero azimuth position is defined to be the 12 o'clock position for blade number 1 (i.e. the position where the trigger signal is given).
- Blade numbering: The order in which the blades pass the tower is for a three bladed turbine: 1,2,3
- Definition of yaw angle, see figure 1.3

2.2.1 Activities and results of Phase 1 (design and tunnel effects)

WP 1: functional specifications
Main Participants: ECN with support of other participants

- After weighting advantages and disadvantages, it was decided to construct a 3 bladed model, the main argument being that the model should be representative of current technology.
- In order to maximise the Reynolds number and still have a sufficiently small Mach number, the tip speed of the model was set at 100 m/s.
- The rotational direction is clockwise when looking downstream to the rotor.
- The maximum number of signals from the rotating systems was decided to be 160, based on 5 Printed Circuit Boards (PCB's), which each accommodate a maximum number of 32 signals each (see also WP5).
- The highest frequency requested for data analysis was set at 1.5 kHz. An expected Strouhal number of 0.1 for the tip region would be correlated with a frequency of approximately 1 kHz. The data acquisition and transfer system was being designed accordingly
- Initially the pressure sensors were all thought to be installed in one single blade. However, it turned out to be impossible to install all PCB's within one single blade, since this would lead to PCB positioned near the mid blade section. At that position, blade deflection would cause the destruction of the PCB's. For this reason the PCB's (and the corresponding pressure sensors) needed to be divided over all 3 blades. The possibility of having the PCB's outside of the blade was discarded since the problem of Electro Magnetic Interference (EMI) would then be such that no guarantee can be given regarding the noise to signal ratio. The number of (Kulite) sensors was finally decided based on the cost price and the available budget, and on the number of total signals that can be taken from the rotating system. This resulted in 148 Kulites.

- The Large Scale Low Speed (LLF) facility of DNW was used in its open test section configuration, with a cross section of 9.5 by 9.5 m^2 , where flow is blowing from a nozzle to a collector (with a closed loop between collector and nozzle).
- The model diameter was 4.5 m
- It was decided to perform PIV measurements of the near turbine flow field, simultaneously with the blade pressure distribution. Initially it was intended to perform these measurements with probes on a so-called wake rig. However, PIV yields the same type of information with a much higher quality in a more efficient way, since a wake rig would be a fragile and intrusive instrument, which would have provided only low resolution data.

WP 2: Navier Stokes and Euler calculations
Main Participants: RISO,CRES,NTUA,ECN,NLR

The purpose of this task was to estimate the blockage effects in an open or closed test section and in this way determine the largest admissible diameter of the model rotor. A rotor diameter of 4.5 m (in the open test section of 9.5*9.5 m^2) was originally considered to be quite acceptable as far as blockage effects are concerned. This expectation was based on first Navier Stokes calculation [12] and on measurements of the drag coefficient of gauzes of different sizes in the pilot tunnel (PLST) and DNW [13]. However, further work indicated more severe blockage effect, mainly in the form of a flow acceleration in the far wake towards the collector, which is due to the conservation of mass between the collector and the nozzle. The results improved the understanding of the physics behind the tunnel effects in an open measurement section considerably but it was realised that this understanding was based on theoretical methods. Though even the best possible methods are used, they still suffer from considerable uncertainties. For this reason the PCC decided to verify the methods and the blockage effects with a further so-called pilot tunnel test [17]. In the pilot tunnel (i.e. a 1/10 scaled down tunnel of the actual DNW wind tunnel) the axial velocity has been measured through hot-wires at several positions upstream and downstream of the rotor.

The main conclusion from the pilot test was that, as expected, clear tunnel effects are found in the far wake. This in turn will effect the induction in the rotor plane to some extent. Nevertheless many indications were found which gave rise to the believe that tunnel effects are limited in the rotor plane:

- The ‘breathing slots’ placed just behind the collector were shown to decrease the tunnel effects. During the pilot test, some tufts on the slot clearly indicated a suction of flow into the tunnel;
- The calculations with a vortex ring model showed a very good agreement between calculated and measured deceleration to the rotor plane;
- Later CFD results on a tunnel without a turbine model, showed that the tunnel effects are partly explained by the development of a jet. As such a relatively easy correction should be possible.

A smaller diameter of the model rotor would obviously reduce the problem of blockage, but the different calculation methods devised to estimate the conditions all showed that no considerable improvement is obtained unless a reduction to approximately half the

rotor size (2 m diameter) were to be chosen. This was not possible on the other grounds, or at least not within the budget available[1].

Moreover it was decided to verify the tunnel effects in the Mexico set-up from pressure transducers which were mounted in the collector walls of the LLF.

WP 3. Aerodynamic design of the rotor
Main participants: ECN, DUT, RISOE with support of other participants

The aerodynamic design of the rotor was based on a 4.5 m diameter rotor.
The profiles chosen for the model are a DU 91-W2-250 airfoil at the root of the blade, a RISØ A1-21 airfoil at mid span and NACA 64-418 airfoil at the outer part of the blade.

The design tip speed ratio was chosen relatively low at 6.5 in order to have a slightly larger chord. The resulting chord and twist distribution are shown in figure 2.1.

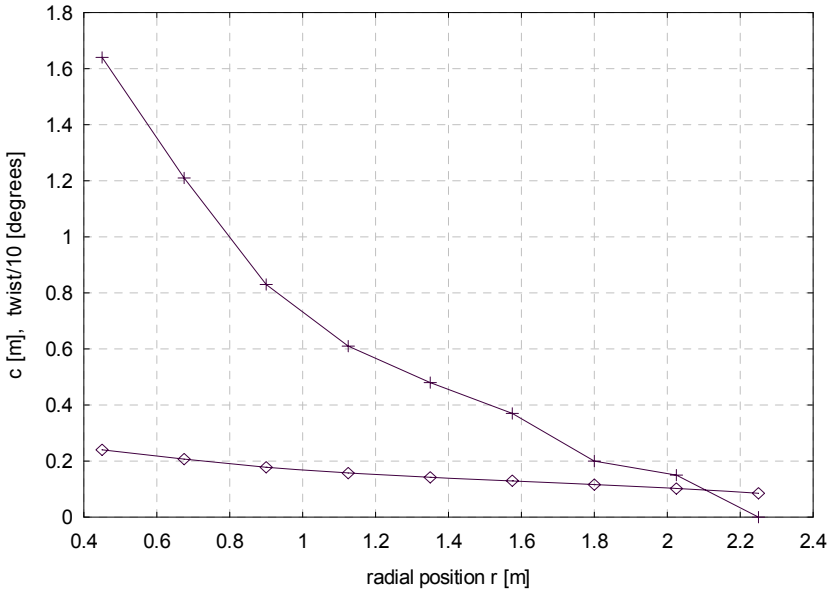

Figure 2.1. Design data of model rotor

The distribution of pressure sensors on the instrumented blade was also defined. The positioning of the Kulite pressure sensors needed some attention (see [9]). Usually the pressure sensors are mounted flush with the surface, but the large number of sensors in the leading edge area would give rise to a facetted surface. The solution was to use cavity mounted sensors, with a pressure tapping of 0.2 mm, at some loss of dynamic response. This option was studied both theoretically and experimentally and showed to maintain the dynamic response upto 1.5 kHz quite well. For this reason this solution was adopted, see also [7].

Moreover it was decided to apply zig-zag tape at 5% of the chord (both at the pressure and suction side) to provoke transition and to avoid laminar separation.

WP 4 Structural Design of the model rotor
Main participants: Technion, ECN

[1] The PCB's that receive the signals from the blades would no longer fit into the blade, resulting in deformation of the signal; the Reynolds number, which is at the lower end of what is acceptable, would reduce by a factor of two.

The structural design was based on calculated loads, which were generated under different operating conditions representing the test matrix, see WP7. The maximum blade loads appeared at the maximum wind tunnel speed of 30 m/s (tip speed ratio $\lambda = 3$) and a yawing angle of 30 degrees, and a loss of load condition under which the rotor speeds up.

The chosen blade material is aluminium; both the external and the internal shape has been produced by numerical milling techniques.

Figure 2.2: Blade manufacturing

The structural layout interacted strongly with the space available and needed for the PCB's. As mentioned in WP 1 it turned out that the PCB's cannot be integrated into one blade without suffering bending. For this reason it was decided to divide the PCB's and the resulting pressure sensors over 3 blades

With regard to the power absorption system, the fundamental choice was made for an electrical system with rapid speed control and the possibility of electrical braking. Furthermore a pitching mechanism was implemented which allowed for fast pitching with pitch angles ranging between -5 and 90 degrees. Regarding the model support, it was decided to use the tunnel balance system (so called external balance), which at the same time allows for the measurement of the three forces and moments acting on the model.

2.2.3 Activities and results of phase 2: preparation of the measurements and data acquisition.

WP 5: Design of the data acquisition system
Main participants: DUT, NLR, Technion

The following instruments were mounted in the model:

- 6 strain gauge bridges on the blades to measure the in-plane and out-of-plane bending moment of each of the three blades
- 1 temperature sensor in one of the instrumented blades

- 148 Kulite pressure sensors divided over 3 instrumented blades
    - The pressure transducers were mounted at 25%, 35%, 60% 82% and 95% span, where the number of pressure transducers per station varied between 25 to 28. The pressure transducers were connected to PCB's (Printed Circuit Boards) in the blade from which the data were led (digitally) over a slip-ring to the data acquisition units in the non-rotating part of the model, using a so-called data grabber. As explained at WP 1, conflicting requirements on the structural needs of the blade on one hand and the required space for the PCB's in the model blade on the other hand, made it necessary to divide the pressure sensors over all three blades (where blade 1 has the instrumented sections at 25% and 35% span, blade 2 is instrumented at 60% span and blade 3 is instrumented at 82 and 95%. A limited number of pressure sensors were mounted at similar locations at the other blades to check the reproducibility of the pressure measurements on the different blades
- 1P trigger sensor. An optical 1P sensor was mounted which generated a trigger signal when blade 1 was passing the 12 o'clock position (i.e. zero azimuth angle).

The raw data sampling rate was 5.5 kHz.

WP 6: Model Construction
Main participants: Technion, NLR, DUT

The following activities were performed within WP6:
- The model components were manufactured. The main model components are the blades, the pitching mechanism, the hub components, the cone and cone extension, the main shaft, the dynamometer and the tower. Furthermore the PCB's had to be manufactured.
- A functional test of the Kulite pressure transducers was done in the wind tunnel.
- The model was instrumented with the Kulites, the PCB's and the additional sensors and preliminary functional tests were made.
- Thereafter the model was integrated and placed on the model support frame, which connects the tower to the DNW external balance.
- Mechanical tests, including static balancing, a rotating functional test and a rotating stability test were performed in the DNW preparation room. The masses, centre of gravities and eigenfrequencies of all blades have been determined. The instrumentation of the blades caused some unbalance, which was corrected by means of counter weights. Thereafter the model turbine experienced a very stable operation with only some vibrations at a rotor speed around 290 rpm (due to a soft tower/balance construction). This was well below the operational rotor speeds of 324.5 and 424.5 rpm and the fast speed control assured a rapid passing of this rotor speed.

An important delay occurred in January 2005 after Technion had completed the manufacturing and testing of most components. During transportation of these components from Technion to DNW, they were severely damaged. After consultation of the Dutch participants NLR and ECN, which inspected the damage, Technion decided to return the damaged wind tunnel model to Israel and repair all damage. This included the replacement of the generator, the slip rings for data transfer, the two main bearings, the pitch mechanism in the hub and part of the hub cladding.

Figure 2.3 shows the damaged model after the accident, figure 2.4 shows the final construction activities in the preparation hall of DNW and figure 2.5 shows the set-up in the test section of DNW.

Figure 2.3: Damaged model

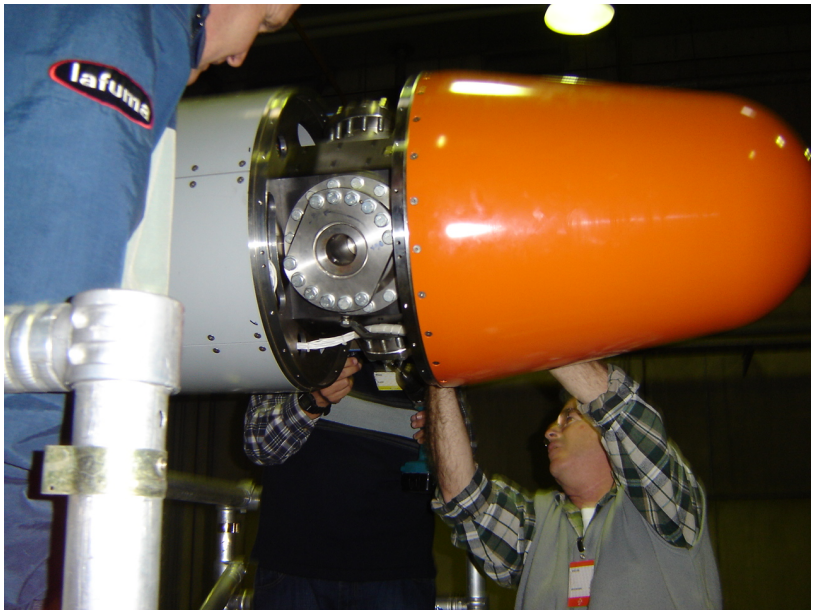

Figure 2.4 Construction activities

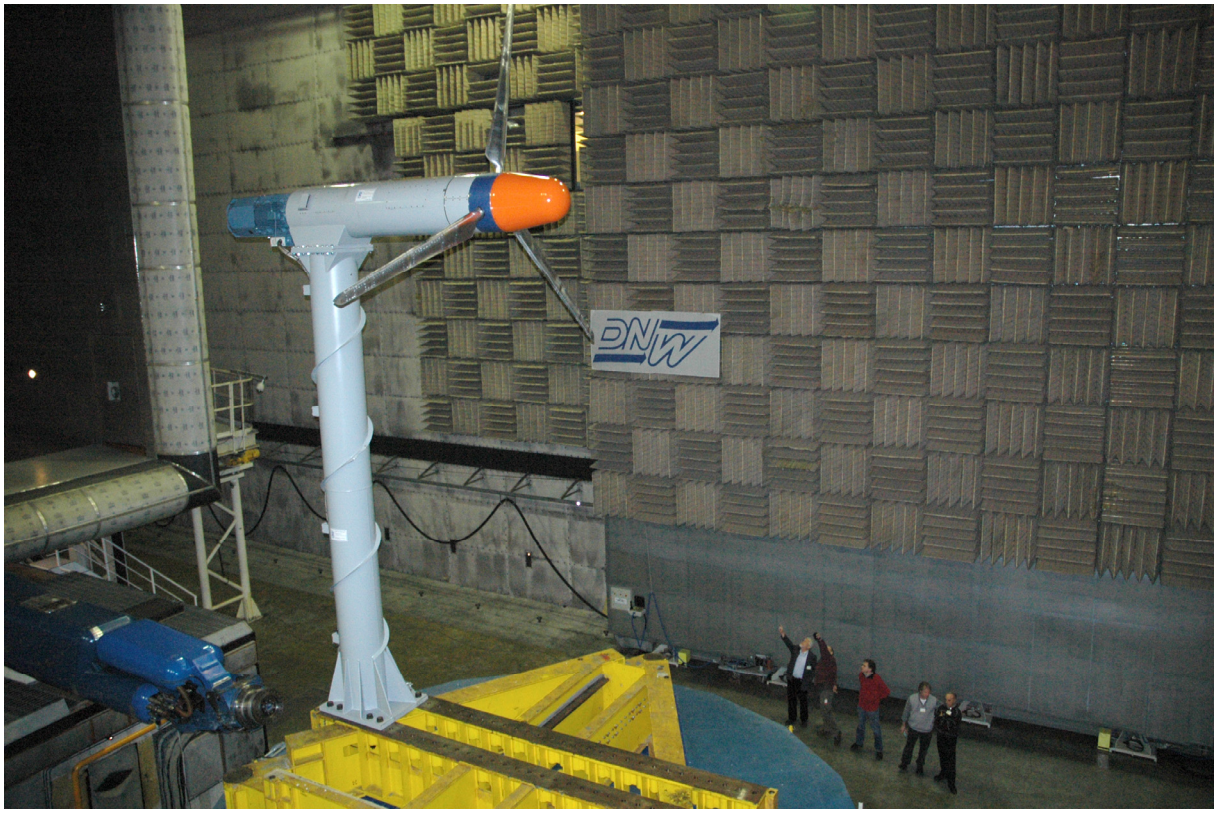

Figure 2.4: Model turbine on balance

WP 7: Experimental matrix definition.
Main participants:RISOE, NLR, DNW, ECN, FOI

An experimental matrix, which defined the measurements in great detail had been prepared before the measurements. It was based on a total of 50 hours of tunnel time (including the installation and the dismantling of the model), which had been subcontracted to DNW. In the preparation of the test matrix the definition of a data point and the measurement period per data point was very important.

- The first data points were without the PIV recordings, hence these data points only include the measurement of the pressure distributions and the blade root bending moments in conjunction with the measurement of the tunnel data (tunnel speed etc). In the sequel these data points are denoted as 'pressure data points'. The next data points included the PIV measurements where the blade and tunnel data were measured simultaneously. These data points are denoted as 'PIV data points'.

- Pressure data points:
  A pressure data point is defined as a recording during which the conditions (in terms of tunnel conditions and model configuration) remained constant (the only exception lies in the dynamic inflow measurements, see below, where a data point includes a step in pitch angle or rotor speed). The pressure and blade root bending moments are sampled with a frequency of 5.5 kHz (effectively 1.5 kHz). In most cases the rotor speed was approximately 7 Hz. This implies that the measurements were taken at every 1.7 degrees angular interval. The measurement period was 5 seconds (i.e. 35 revolutions for a rotor speed of 7 Hz). It is noted that the tunnel data (tunnel speed, pressures, temperatures) and the balance data were averaged over the data points.
  Pressure data points have among others been taken at axi-symmetric conditions for a large variety of tunnel speeds, pitch angles and two rotor speeds. Furthermore pressure data points have been taken at yawed flow, dynamic inflow and parked conditions.
- PIV data points. A PIV data point is defined as the measurement of a flow vector field within a PIV sheet (see below) during which the conditions in terms of tunnel conditions and model configuration remained constants. A data point is composed of 100 'frames' where a 'frame' is the result of two subsequent photographs (see below). The frames are all made at a given blade position ('Phase locked'). The sampling frequency between two frames is approximately 2.4 Hz, which enables a 'phase locked' measurement (note that the rotor speed was 7.075 Hz). The resulting measurement period for a PIV data point in then in the order of 40 seconds.
  PIV data points have been taken under axi-symmetric conditions (3 tunnel speeds) and yawed conditions (1 tunnel speed).

Intermezzo: Description of PIV measurement technique

- The PIV measurements were performed in the following way:
  - A PIV traversing tower with two camera's focussed on a PIV sheet (337*394 mm) in which the flow field is measured. The PIV sheet is located horizontally in the symmetry plane of the rotor at the 270 degrees azimuth position (i.e. at the 9 o' clock position).
  - The PIV tower was mounted on a traversing mechanism, which made it possible to traverse PIV sheets in a horizontal plane where the range in axial direction is approximately 10 meters and the range in radial direction is approximately 1.2 m (see below).
  - Seeding (in the form of small bubbles) was introduced in the settling chamber, upstream of rotor.
  - The seeded PIV sheet is illuminated with a strong laser flash, and two digital photographs are taken with a delay of only 200 nanoseconds and a comparison is made between the two 'seeding fields';
  - The PIV sheet is then subdivided into small 'interrogation windows' and a large number of velocity vector fields are 'attempted'. The actual velocity vector is the one resulting in maximum cross correlation between the two 'seeding fields'

The test matrix is discussed in more detail at WP11

WP 8: Preparation Flow visualisation

In the original work plan, flow visualisation activities have been defined. Activities which have been proposed were smoke, tufts, and liquid crystals etc.

With regard to this phase, only exploratory studies of possibilities have been conducted. There after this task was skipped due to the fact that PIV is a very good alternative for most of the originally scheduled flow-visualization activities.

WP 9: Wake rig

In the original work plan, the wake was expected to be measured with a so called wake rig, i.e. a rig with many devices to measure the flow field. Eventually it was decided to reject the wake rig, since most of the information, which is expected from this wake rig, can also be obtained from PIV.

2.2.3 Activities and results of phase 3: Measurements.

WP10: Two dimensional profile measurements
Main participants: DUT

The two-dimensional aerodynamic characteristics of the blade-root airfoil DU 91-W2-250 and the tip NACA 63-418 airfoil were measured extensively in the wind tunnel of Delft University at Reynolds number between 400,000 and 1,000,000, see [24] and]25]. These 2D airfoil data serve as a reference to the rotating measurements. The angle of attack ranged between -30 to 40 degrees. Tests were conducted not only in the clean configuration, but with 3 different locations of the roughness (zigzag) tape as well.
The tests were performed both with the measurement of surface and wake pressures and with the balance system.

WP11 Measurements in a large wind tunnel, including flow visualization
Main participants: NLR ,DNW, Technion, DUT, ECN

The measurements in the DNW LLF wind tunnel were carried out in the period from December 6 to December 14 2007.

The test matrix (as defined in WP7) was followed in a very strict way and although it was designed to be overloaded, it was even possible to perform a few additional non-planned measurements within the 50 hours of tunnel time which were subcontracted to DNW.

As a result, 944 data points could be taken at the following configurations and conditions:

- Pressure data points: The first 257 data points were taken without the PIV recordings. These measurements were done for the following conditions:
  - Axisymmetric conditions
    - Rotor speed: 324.5 rpm and 424.5 rpm (V_{tip} = 76 and 100 m/s or 5.35 Hz and 7 Hz)
    - Tunnel speed: Between 5.5 to 30 m/s
    - Pitch angles: Between -5.3 and 1.7 degrees

- Yawed conditions: Measurements have been performed at yaw angles of 15, 30 and 45 degrees and tunnel speeds of 10, 15, 18 and 24 m/s. The pitch angle = -2.3 degrees
- Dynamic Inflow: Fast pitching steps and rotor speed steps have been measured at tunnels speeds of 10, 15, 18 and 24 m/s. It must be noted that the pitch angle was not measured directly but the start and end values were recorded. The pitch angle varied between -2.3 and +5 degrees. This pitching step was supposed to take place within 0.05 seconds. The rotor speed was derived from the 1P trigger sensor.
- Parked rotor measurements. Parked rotor measurements have been done at a tunnel speed of 30 m/s and pitch angles ranging between -2.3 and 90 degrees

- PIV data points (Note that the PIV measurements were combined with measurements of the pressures and the blade root moments). Approximately 700 PIV data points have been taken for the following conditions:
  - Axi-symmetric conditions at a tunnel speed = 10, 15 and 24 m/s, a rotor speed of 424.5 rpm and a pitch angle = -2.3 degrees Furthermore measurements have been performed at pitch angles of -5.3 and 0.7 degrees and a tunnel speed of 24 m/s. The following traverses have been made:
    - Two radial PIV traverses from r = 1.374 m to r = 2.54 m (i.e. from r/R = 0.61 to r/R = 1.29) at x = -0.15 and x = 0.15 m (i.e. at x = 0.066 R upstream and downstream of the rotor plane). It is noted that these locations refer to the PIV sheet centers. The radial traverses are performed at 6 blade azimuth positions with a 20 degrees azimuth interval (where the 3P flow dependency makes it sufficient to cover only 120 degrees azimuth).
      It is noted that these radial traverses are <u>not</u> made for pitch angles of -5.3 and 0.7 degrees.
    - Two axial traverses from x = -4.325 m to x = 5.725 (i.e. from 1.92 R upstream of the rotor to 2.54 R downstream of the rotor at r = 1.374 m and y = 1.845 m (i.e. at r/R = 0.61 and r/R = 0.82). The locations again refer to the centres of the PIV sheet. The traverses are made for 1 blade azimuth position (in most cases the measurements were done for zero azimuth of blade 1);
    - Vortex search: For a given blade azimuth angle (usually 270 degrees azimuth of blade 3), the position of the tip vortex is searched by 'trial and error' at a large number of axial positions.
  - Yawed conditions: Yawed measurements have been performed at yaw angles of plus and minus 30 degrees and a tunnel speed of 15 m/s, where the pitch angle = -2.3 degrees. Both axial and radial traverses have been performed in a procedure very comparable to the procedure as described at aligned conditions. The locations of the PIV sheets were also more or less similar. Furthermore a vortex search has been carried out.
    In view of the fact that the PIV sheets were located in the horizontal symmetry plane at an azimuth angle of 270 degrees, the measurements at the plus and minus yaw angle represent the flow field at two opposite azimuth angles (90 and 270 degrees) for the same yaw angle.

WP12 Data processing and interpretation
Main participants:NLR,DNW

Quick-look software had been developed, which processed the raw pressure data almost on-line into preliminary pressure distributions and into the aerodynamic force coefficients |(averaged over a 60 degrees azimuth interval). This allowed a first assessment of the data, which among others showed the necessity of frequent zero runs due to the zero drift of the sensors and the need for a repair/modification of the 1P sensor. The tunnel balance data could also be inspected on-line.

The PIV data were presented by DNW in the form of preliminary vector plots in an almost on-line manner. This was a unique feature of the DNW facility and it was an important pre-requisite to make the on-line vortex searching possible.

WP13 Data archiving into a database
Main participants: NLR, DNW, ECN
The data (100 Gbytes) are stored on external hard discs and distributed between the participants. On the disc, the time series of pressures and strain gauges are given in raw form. Furthermore some processed data in the form of azimuthally averaged pressure distributions and profile coefficients (azimuth interval 60 degrees) are stored in ASCII format. Moreover the disc contains a data point overview and the basic software with which the raw pressure data can be processed.
The PIV data are given in processed form (i.e. ASCII data of the velocity vectors at different x-y-z positions).

2.2.4 Activities and results of phase 3: Analysis.

WP14 BEM adaptation
Main participants: ECN, DTU
As mentioned before, the measurements were executed in the week from December 7, 2006 to December 14, 2006 where the project end time was December 31, 2006. This left very little time for comparing model results with measured data. Nevertheless some activities on this WP could be performed prior to the measurements.

1. Evaluation and development of tip loss techniques [24];
2. Analysis of basic assumptions in the BEM technique
3. Developing an extended BEM code for modelling wind turbines in wind tunnels [15];

In the table below a comparison is given between the BEM calculated axial force on the rotor shaft and the measured axial force on the tower foot for a pitch angle of -1.2 degrees (note that the calculations are performed for a slightly different pitch angle of -1.3 degrees). It is noted that the calculated axial force does not include the drag from the tower which is a rather uncertain quantity in view of the fact that the Reynolds number based on the tower diameter is close to the critical Reynolds number (in the order of $3\ 10^5$). A large part of the under prediction is then expected to be caused by this tower drag. Some indication of the tower drag can be found from the balance measurements at parked conditions, which have been performed at a tunnel speed of 30 m/s and different pitch angles. The minimum axial force appears to be in the order of 1600 N. At this pitch angle it is expected that the rotor loading is low and that the axial force on the balance is dominated by the tower drag (this assumption obviously needs to be assessed more thoroughly). Table 1 anyhow shows the under prediction

in axial force to be much less than 1600 N and as such the missing tower drag cannot be excluded as explanation of the differences.

V_{wind} (m/s)	F_{ax} (measured at tower foot) (N)	F_{ax} (calculated at rotor shaft) (N)
10	1039	945
15	1979	1686
18	2487	2019
24	3285	2187
30	4091	3243

Table 1: Comparison between calculated and measured axial force (θ = -1.3 degrees). Note that the tower drag is not included in the calculations.

It can furthermore be mentioned that the analysis of data, as described in the appendices A and B will definitely provide important information for the validation and improvement of BEM models. The PIV traverses in axial direction allowed, for the first time ever, a detailed appraisal of the development of the induction upstream and downstream of the rotor, which forms important input to a BEM model. Near the 60% station, strong trailing vortices have been measured which disturb the commonly assumed smooth behaviour of the velocity decay considerable. Once completely understood it can be used to modify BEM models in regions where large gradients occur of the bound vorticity on the blade.
Important information on the refinement of BEM tip correction models is obtained from the induction field which is measured between the blades. This does not only allow a refinement of tip correction models at aligned flow but even for yawed flow.

WP15 Engineering rules for the effects of boundary layer manipulators.
Already at the start of the project, these activities were given a low priority (in view of the fact that the relevance of these manipulators has become less) and they were cancelled by which the unforeseen and crucial Pilot Tunnel test became possible(see WP2).

WP16 Limited validation of Navier Stokes solvers.
Main participants:RISO, FFA, ECN

The same remark as given at WP14 applies, i.e. time was too short for a thorough evaluation using Navier Stokes Solvers. Nevertheless some activities have been performed by RISØ.
Preliminary CFD computations of the MEXICO rotor have been performed. Based on the blade description provided by Technion, an 8-block mesh was constructed around the MEXICO rotor. Using standard meshing approach, a topology with five inner blocks and three outer blocks were chosen, exploiting the 120 degrees symmetry of the problem. The mesh spacing is approximately $1 \cdot 10^{-5}$ at the blade surface, and the outer boundary is located 6 rotor radii's from the rotor centre. The influence of the tunnel is neglected in these computations and the undisturbed velocity is specified at the inlet part of the outer boundary. Five wind speeds are computed [7, 12, 15, 20, 30] m/s, assuming a density of 1.225 kg/m^3, a viscosity of $1.78791 \cdot 10^{-5}$ and 425.5 RPM. Both time true and steady state computations are performed. The calculations have been done for a pitch angle of zero degrees. No measurements were done at this pitch angle but it is important to realise that the work performed in this activity can be considered as preparation activities for future NS calculations.

Wind Speed [m/s]	Mechanical Power [kW]
	CFD
7	0.3
12	7.6
15	14.9
20	29.0
30	36.8

Table 2: Mechanical power computed by the initial CFD computations at pitch angle of zero degrees

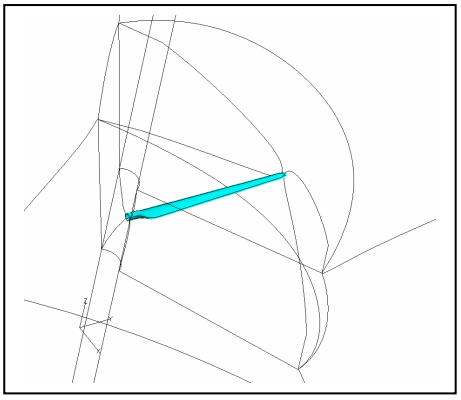

Inner five-block topology around the Mexico blade.

It can furthermore be mentioned that the analysis of data, as described in the appendices A and B yields important information for the validation and improvement of advanced flow solvers, like free vortex wake models and Reynolds Averaged Navier Stokes solvers. It has among others been possible to determine the velocity decay in the wake, the tip vortex transport velocities, details of the tip vortices viz. the vortex core diameter and the maximum rotational speed within a vortex, and the viscous wake shed by the blade. It has furthermore been possible to relate the bound vortex strength to the tip vortex strength.

WP17: Reporting
The reports which been prepared will be described in the list of deliverables, see section 3.1

WP18: General co-ordination during the entire project duration.

Management aspects will be discussed in section 3.3

2.3. Assessment of results and conclusions

The most important results from the project are:

- An extensively instrumented wind turbine model. This model can be used for future wind tunnel experiments and/or field experiments.
- A database of unique detailed aerodynamic measurements on a representative wind turbine model taken in the largest wind tunnel of the EU. The data (100 Gbytes, i.e. more than 270000 data files) are organised in a self explanatory way on external hard discs and distributed between the participants. On the disc, the time series (of pressures and strain gauges) are given in raw form. Furthermore some processed data are stored in ASCII format. The disc also contains a data point overview and the basic software with which the raw time series can be processed.
  The PIV data are given in processed form (i.e. ASCII data of the velocity vectors at different x-y-z positions).
- In view of the fact that the measurements have been taken from December 6 until December 14, 2007 where the end date of the project was December 31, 2007, only very little time was left for analysis of data. Nevertheless quality assessment of the data could be performed and some first very important new insights on the flow field around the rotor have already been gained. In the near future these new insights will definitely help to validate and improve aerodynamic wind turbine models:
  - The PIV traverses in axial direction allowed, for the first time ever, a detailed appraisal of the development of the induction upstream and downstream of the rotor. This is important information for BEM codes, CFD codes and free wake models. A comparison between the measured slow down of the velocities in the wake and a theoretical estimate shows a very good agreement at 82% span but a poor agreement at 61% span which is due to the release of strong trailing vorticity near that location. At higher thrust coefficients, clear indications have been found for increased turbulent activity, which is most likely related to the turbulent wake situation.
  - Some very unique details of the tip vortex could be made visible. The measurement of the v-component formed a perfect basis for such study and enabled the determination of the vortex core diameter and the maximum rotational speed in the wake of a wind turbine. This definitely will help to improve free vortex wake models.
  - The bound vortex strength has been estimated using the measurements of the pressure distributions along the blade. The estimated value compares very well with the tip vortex strength measured with PIV. This is again very important information for free vortex wake models.
  - The tip vortex trajectories could be determined. A clear expansion is found which is largest for the lower tunnel speeds. The resulting transport velocities of the tip vortices do not seem to decrease with downstream distance. This is contrary to some intuitive models, which assume that the transport velocity is the average of the wake speed and the undisturbed outer speed.
  - For the first time ever, it has been possible to measure the induction between the blades. Towards the tip, these measurements can be used to refine tip correction models, even for yawed flow.
  - For the first time ever, the velocity field from the viscous wake which is released from a rotor blade has been measured. This is important information

for all types of wind turbine codes.

- The pressure distributions at 60% span and a tunnel speed of 24 m/s show the expected behaviour: At aligned flow, they indicate an axi-symmetric flow (i.e hardly any azimuthal variation in pressure distributions is found) and they indicate a stalled boundary layer, as expected at this high tunnel speed. At yawed flow, the pressure distributions show a cyclic stalled/unstalled variation.
- The response of the normal force to the rotor speed ramp does show an overshoot.
- A preliminary c_n-α curve has been derived at parked conditions, which at least for some sections, compares reasonably well with the expected 2D airfoil characteristics.
- With regard to the quality of the data the following preliminary conclusions were drawn:
    - The PIV measurement give a very detailed and consistent picture of the flow field, in terms of induction, vortex transport velocities, vortex structures where even the velocity field from the viscous wake which is released from a rotor blade could be measured. The analyses, which have been performed, were a testimony for the great flow detail present in the PIV measurements.
    - Generally speaking the pressure distributions at 60, 82 and 92% span look reliable. This is confirmed by a good to reasonable agreement between the pressures at the different blades (and similar positions). The good quality is also confirmed by a good repeatibility of the data. Repetition runs indicated hardly change in pressure distributions, even after 1 week. This is illustrated in figure 2.5 where the pressure measurement at 82% span is shown for similar conditions at a data point (nr 117) collected in the beginning of the tunnel slot and a data point (nr 929) at the end of the tunnel slot almost 1 week later. The difference in pressure distribution turns out to be very small.
      The pressure distributions at 25% and 35% do not always comply with the expectations. It is suspected that this is due to a slight instable behaviour of the Kulite pressure transducers in combination with very low pressures at the inner part of the blade. It is noted that frequent zero runs have been carried out due to zero drift, but this drift could be a substantial fraction of the pressures at the inner part of the blade. In figure 2.6 the repetition of the pressure distributions at the 35% span is shown. The figure indicates that 4 pressure transducers might be malfunctioning at data point nr 117.
    - The response of the normal force to the pitching ramp leads to the suspicion that the ramp is somewhat slower than specified.
    - The blade root bending moments seem reliable on two blades. The (less relevant) moments on the third blade look less reliable which is due to outliers in the calibration.
    - The balance data give a consistent picture of the loading at the tower foot although it is suspected that a few loads are in the lower end of the measurement range.

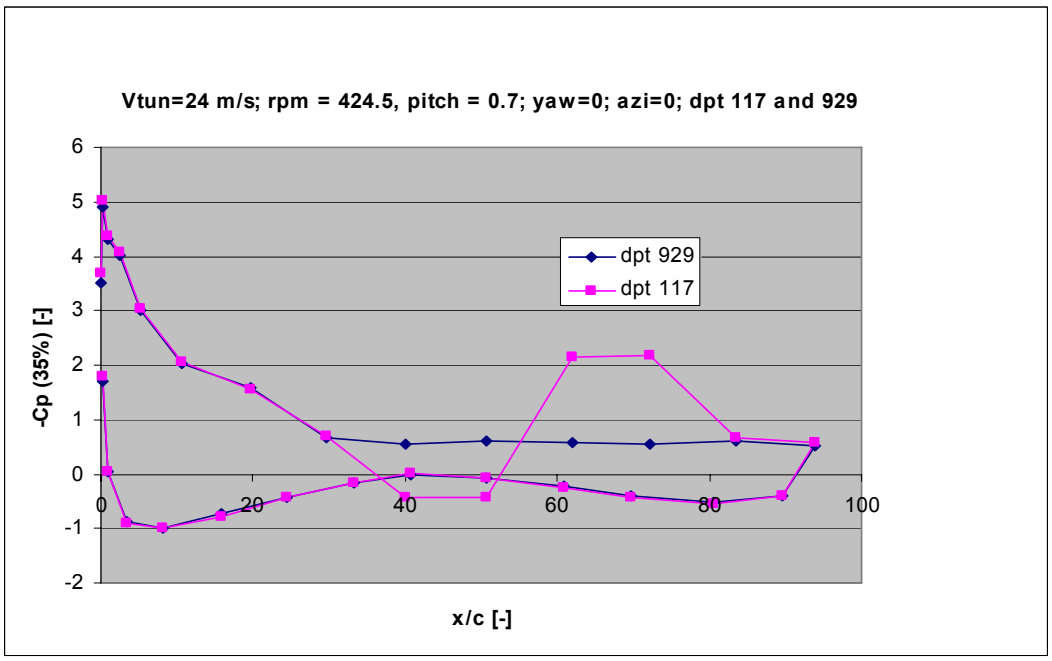

Figure 2.5: Comparison of pressure distribution at 35% span at two different data points.

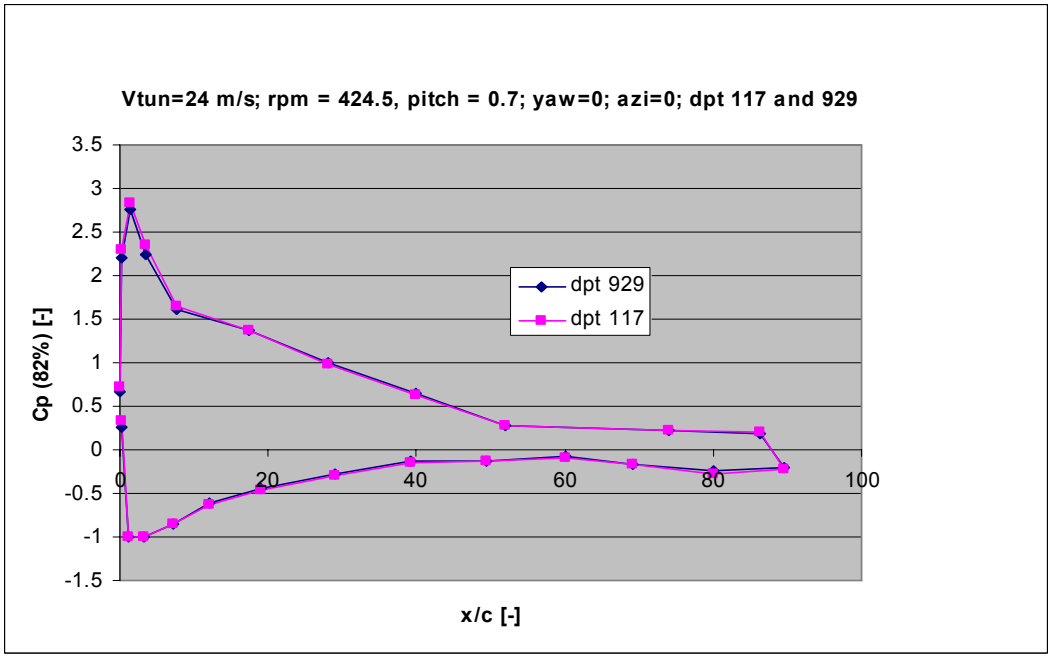

Figure 2.6: Comparison of pressure distribution at 82% span at two different data points

This then leads to the most important conclusion of the project, saying that a high quality database is created of measurements in the largest wind tunnel of the EU, which are taken under a large variety of conditions. This will serve the wind community for many years to come as a basis for further model improvement and validation.

2.4 Acknowledgement

The financial support from the EU 5th Framework programme is greatly acknowledgement. Furthermore the Dutch contribution in the project was partly financed by SenterNovem, an agency of the Dutch Ministry of Economic Affairs, under the TWIN programme. The contract number was 0224-01-57-21-0013.

2.5 References

[1] H. Snel et al: Annex I: Description of Work for Mexico Project, NNE5-2000-00163
[2] J.G. Schepers et al: Verification of European Wind Turbine Design Codes, VEWTDC, ECN-C-01-055, April 2002
[3] H. Snel: Mexico WP1: Baseline Definition, Mexico-Doc-WP1-01-01, ECN, June 11,2001
[4] C. Bak et al: Mexico WP7: Detailed experimental matrix, Mexico-DOC-WP7-01-01, RISØ-I-2216, October 2004
[5] S. Voutsinas et al: Mexico WP2: Navier Stokes and Euler Simulations to determine the maximum rotor size, DOC-WP2-01-01, NTUA Greece, November 2003
[6] H. Snel: Mexico WP3: Aerodynamic Pre-design and loads for the Mexico Model rotor, ECN, August 10, 2001
[7] J.G. Schepers: Minutes of 4th Progress Meeting, Held on June 17, 18, 2002 at DUWIND, DUT, Delft The Netherlands. DOC-MIN02-02
[8] J.G. Schepers: Minutes of task meeting , Held on March 19, 2002 at NLR, Amsterdam ,The Netherlands. Doc-Min 02-01
[9] W.A. Timmer: Task Report: Location of the pressure sensors. March 2002. DOC WP3-02-01
[10] H. Snel: Minutes of task meeting, held on January 22-24, 2003 at DNW, Marknesse, The Netherlands, DOC-MIN03-01, February 2003
[11] A. Rosen et al: Model design, Technion, Israel, August 2003
[12] J.G. Schepers: Minutes of progress meeting, held on June 28,29 at RISO, Roskilde, Denmark, DOC-MIN01-02, July 2001
[13] W.Z Shen and J. Sorensen: Actuator line simulations of wind tunnel blockage, MEK-AFM-Mexico 01, DTU, March 2002
[14] H.A. Madsen and Christian Bak: Flow calculations on different wind tunnel configurations using an actuator disc model, RISO-I-1764(EN), DOC-WP2-01-02
[15] Sørensen, J.N., Shen, W.Z. and Mikkelsen, R. (2004) "*Wall Correction Model for Wind Tunnels with Open Test Section"*. Proc. of 'The Science of Making Torque from the Wind', Editor: G.A.M. van Kuik, TUDelft, pp. 196-202
[16] G. Hermans: Specificaties Mexico Data Acquisitie Systeem (in Dutch with English addendums), GED002, Technical University of Delft, November 2006
[17] Doeke Rozendal: Flow field measurements on a small scale wind turbine model in the DNW PLST wind tunnel, NLR-CR-2003-485
[18] H. Snel and G. Schepers: Mid-Term Assessment report for Mexico Project, NNE5-2000-00163, August 2003
[19] G. Schepers: Minutes of progress meeting, held on February 15-16,2001 at ECN, Petten, Holland, DOC-MIN01-01, March 2001
[20] J.G. Schepers: Minutes of task meeting, Held on September 12 and 13, 2001 at DNW, Marknesse, The Netherlands, Doc-Min 01-03
[21] G. Corten, H. Snel and G. Schepers: Minutes of progress meeting, held on November 27-29, 2001 at NTUA, Athens, Greece, DOC-MIN01-04, December 2001
[22] J.G. Schepers: Minutes of Design Review Meeting, Held on July 2-3, 2003, at ECN Holland. Doc-Min03-02
[23] J.G. Schepers: Minutes of MTA/Plenary meeting, Held on August 27/28, 2003, at FOI Sweden. Doc-Min03-03

[24] Shen, W.Z., Sørensen, J.N. and Mikkelsen, R. (2004) "*Tip Loss Correction for Actuator/Navier-Stokes Computations*". Proc. of 'The Science of Making Torque from the Wind', Editor: G.A.M. van Kuik, TUDelft, pp. 138-144

[25] N. Timmer Experimental two-dimensional aerodynamic characteristics of airfoil DU 91-W2-250 at low Reynolds numbers. Report WE 07201, February 2007 Delft University of technology, The Netherlands
Netherlands

[26] N. Timmer: Experimental two-dimensional aerodynamic characteristics of airfoil NACA 64-418 at low Reynolds numbers. Report WE 07202, February 2007 Delft University of technology, The Netherlands

[27] A. Wolf: Rotor speed control system, Technion report, February 2007, Technion, Israel

3. MANAGEMENT FINAL REPORT

3.1 List of deliverables

It is noted that most of the reported deliverables can also be found on the CD which belongs to this report.

Deliverable Number	Deliverable Title	Type	Status	Dissemi-nation Level
1	R: Technical specs of the model	Report	Completed [3]	PU
2	R: Description of exp. Matrix and use of quantities	Report	Completed [4] and [16]	PU
3	R: Calculated wall tunnel effects	Report	Completed [5], [13], [14],[15]	PU
3a	R: Report on pilot test	Report	Finished [17]	PU
4	R: Geometry of the rotor blades	Report	Completed [6] and [9]	PU
5	R: Specs for rotor speed control	Report	Completed [27]	PU
6	R: Structural model design	Report(s)	Finished, [11]	PU
7	P: Data transmission unit	Hardware	Completed	CO
8	P: Data acquisition hardware and software	Hardware and software	Completed	CO
9	P: Model rotor	Hardware	Completed	CO
10	R: Documentation of rotor and signals	Report	Finished [16]	PU
11	R: Runbook for the experiments	MS-Excel sheets	Data point overview is added to external hard disc	PU
12	R: Description of flow viz experiment to be performed	Report	superfluous	PU
13	R: Flow visualization results – smaller tunnels	Report	superfluous	PU
14	R: Calibration reports flow field probes	Report	superfluous	PU
15	R: 2D Aerodynamic properties	Reports	Finished [25] and [26]	PU
16	R. Mid-term Technological Implementation Plan	Report	Finished [18]	PU
17	P. Raw data and video tapes of measurement sessions	External hard disc	Finished on external hard disc	CO
19	P: DVD with measured and processed data	DVD	Finished	CO
23	R: CD containing all project documents	Report on CD	Finished	CO
24	Dissemination report	This report	Finished	PU
25	Data base on external hard disc	External hard disc	Finished	CO

As a result of the fact that the project end time was December 31, 2007 where the measurements took place between December 6 and December 14, 2007 there was little time for analysis of data.
For this reason the following reports could not be delivered

18	R: Report with data description and interpretation	Report	PU
20	R: Description of renewed BEM models and comparisons	Report	PU
21	R: Calibrated engineering models boundary layer manipulators	Report	PU
22	R: Results from limited NS validation	Report	PU

In this respect it should be mentioned however that the project consortium has prepared plans for analysis activities after the project end data and that part of the intended content for deliverable 18, 20 and 22 is reported in section 2.2 at WP14 and 16. This includes a limited comparison between measurements and BEM models and insights which will be used to improve BEM models (relevant for deliverable 20). Furthermore a limited comparison between measurements and NS codes is prepared together with new insights to improve free wake and NS codes (relevant for deliverable 22). It should also be mentioned that reference [15] forms part of deliverable 20: It gives a correction method for the tunnel effect on the momentum part in the BEM method.

It is finally noted that deliverable 21, i.e. a report on calibrated engineering models boundary layer manipulators has been cancelled already in an early stage of the project (in view of the fact that the relevance of these manipulators has become less), see the description of WP15 in section 2.2.

3.2 Comparison of initially planned activities and work actually accomplished

Almost all initially planned activities have been accomplished. Obviously most important is the creation of the base of high quality data, taken in the largest wind tunnel of the EU under various controlled and constant conditions. As a matter of fact the data are of an even higher quality than originally anticipated which is due to the fact that the PIV measurement technique became available, where originally the flow field data was intended to be measured with a wake rig. This would have led to a much poorer quality of data because of the limited resolution and because of the heavy intrusion from the wake rig. It can also be mentioned that much more information on tunnel effects has become available due to the fact that the unforeseen pilot tunnel test has been performed.

The analysis of data and the comparison between calculations and measurements has been more limited than anticipated. This is due to the fact that the tunnel slot became available only 2 weeks before the project end time. Nevertheless some first insights could be gained.

3.3 Management and co-ordination aspects

The project has suffered from severe management problem, see also section 2.2.1. The bankruptcy of Aerpac and Polymarin led to unforeseen co-ordinator activities: Negotiations with potential substitutes needed to be carried out and the workplan and the

budgets needed to be revised. Unforeseen co-ordinator activities were also needed because of the technical delays and because of the accident which happened with the wind tunnel model. This again led to workplan and budget revisions. As a result a total of 5 contract amendments were needed, where eventually, the total project period turned out to be 6 instead of 3 years. Despite all problems, the motivation of the consortium never slacked and all participants remained convinced of the usefulness of the results. Many participants suffered severe project deficits, see Appendix C, which needed to be found from internal funds. As an example the repair of the model can be mentioned which needed to be carried out after the accident. This led to high costs for Technion, ECN and NLR. Although the transport of the model was insured, until now the insurance company has not reimbursed the damage yet, and the costs are, at least temporarily borne by the participants.

The Consortium Agreement was finished in 2002 and signed by all participants. A special point was the role of the National Renewable Energy Laboratory of the USA (NREL), who is not a co-signatory of the project, but whose role is defined in the Consortium Agreement. A bilateral agreement between ECN and NREL has described the rights and obligations of NREL as a participating observer.

Communication between participants took place through the conventional channels, i.e. email, telephone etc but furthermore a number of 5 plenary project meetings and several task meetings took place. Detailed minutes of every meeting are prepared, see [7], [8], [10], [12], [19], [21], [22], and [23]. All project information was stored on a password protected internet site.

Appendix A: Analysis of PIV data (Provided by Bjorn Montgomerie from FOI)

1. Objectives

The aerodynamic testing of the model rotor is useful for a number of scientific and engineering needs. The present investigation was carried out with the limited purpose to compare some fundamental theorems about vortices and how well the PIV velocity information agrees with the nominal wind tunnel velocity.

2. Vortex Analysis and Related Questions

Scientists Helmholtz and Kelvin went through the same lines of thought when they studied vortices independent of each other. The fundamental theorems say that a vortex line in a continuous medium must be a closed loop and its strength does not change along its full length. There is no statement on the shape of the loop however.

Examples of closed loop vortices are vortex rings (smoke rings), the vortex system attached to a flying airplane wing and a corresponding vortex system created by propellers and wind turbines. The three latter vortex systems have the commonality that there is a vortex bound to the wing/blade and the rest of the closed loop consists of trailing vortices, drifting downwind, and being joined at a far downwind position. That position is the takeoff place for the airplane and the starting position for e.g. the wind turbine – with due consideration of the wind drift. Reality, including viscous effects, will make sure that the start connection of the vortices dies out very soon and does not exist after say a minute.

Despite the real lack of a closed loop connection at the far beginning the basic theorems remain the basis for the development of methods implemented as computer code for design and analysis of airplanes, propellers and wind turbines, albeit they coexist with other methods with the same purpose.

The preliminary investigation, which is the background of this topic of the text, aims at finding the deviation between the Helmholtz/Kelvin theorem and "reality", in this case, represented by a model wind turbine with a diameter of 4.5m and the large subsonic DNW wind tunnel driving the turbine in an open test section.

A consequence of the Helmholtz/Kelvin theorem is that it could be expected that the maximum strength of the bound circulation on the blade should be equal to the strength of the vortex that trails behind the tip of that same blade. The blade has a variable load along its active length from root to tip. This corresponds to a variable vortex strength likewise. Vortex strength is measured in a quantity called "circulation", which has the dimension m^2/s. Circulation thus has a maximum, in rare cases two maxima, somewhere along the blade.

The tests allow the evaluation of the pressure, in many points on the blades, to be converted to the so called bound circulation. The PIV velocity sheets capturing a cross section of a trailing vortex can be used to evaluate the circulation of the trailing vortex. Is the circulation of the bound and trailing vortices equal? – A preliminary answer is given by the test data and the human treatment of these data as seen in the following sections.

3. Selections from the Tests

Two sequences including PIV sheets covering the trailing vorticity and a series of PIV takings starting in the stream tube enclosing the turbine disk far ahead ending far behind the turbine, constitute the foundation of the following treatise.

3.1 The Tip Vorticity Sequence

Choosing a case, demonstrated by the figure below and some additional data, allowed the evaluation of the circulation valid for the free trailing vortices.

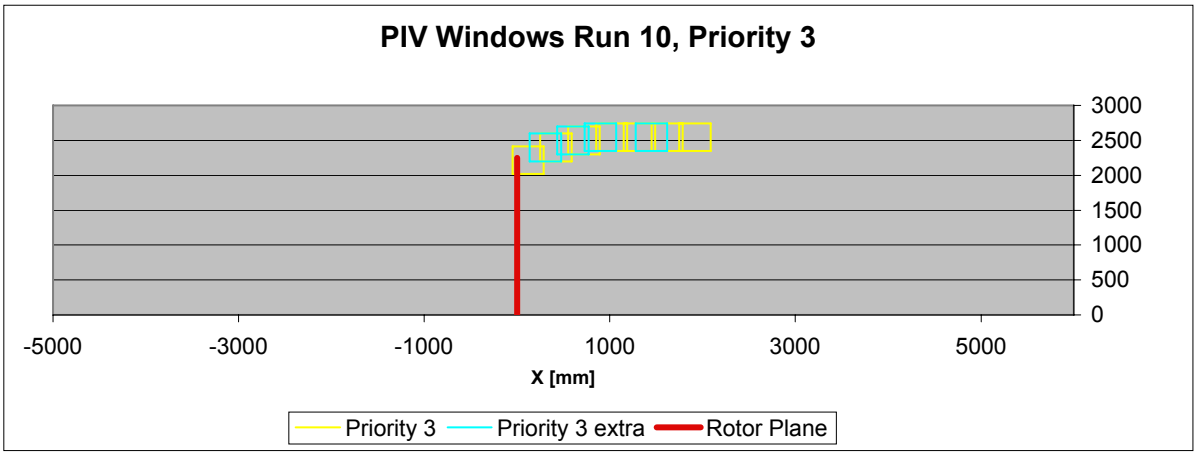

The schematic figure shows the tunnel test section from above. The thin outlines represent the PIV sheet positions. The wind blows from the left. Computer code was developed to plot arrows indicating the direction as size of the wind field enclosed by a PIV sheet. After viewing the PIV sheet in this form the center of the free vortex could easily be seen. Using it as a center for circles these circles were chosen to be the closed path, which is the integration path for the circulation integral. Since the vortex can be modeled as a bundle of many infinitesimal fibers. These fibers appear, in the two-dimensional view, as concentrated near the center gradually thinning out at increasing radii. The circulation calculation is carried out by implementing any suitable method, which is capable of solving the following circulation integral.

$$\Gamma = \oint \mathbf{v} \circ d\mathbf{s} \qquad (1)$$

The expression can be interpreted in words as follows. The closed path **s** (circle) is divided into small straight segments on which the local velocity vector is projected. The length of the projected vector is multiplied by the length of the small segment to give a contribution to the total sum. Applying this method walking around a circle, enclosing a bundle of vortex fibers, will then result in the sum of circulation strengths of all infinitesimal fibers that were circumscribed by the integration path. When the radius of the integration path circle is increased it will enclose more infinitesimal vortex fibers. Consequently this integral will yield a higher value than the previous one.

Proceeding in the described manner for several circles, starting from a very small radius, should thus be expected to result in increasing circulation values, with the added expectation that the curve eventually reaches an asymptotic value when all infinitesimal fibers have been enclosed.

The computer code that was constructed to evaluate circulation was based on the ideas described. A PIV sheet was chosen whose coordinates were: From 13 cm to 47 cm downstream and from 2.20 to 2.59 m of radial extent. It is one of the sheets seen in the figure above. The vortex center was found to be at xc = -0.284 yc = -2.383. The minus signs merely reflect the slightly disturbing fact that the PIV sheet coordinate system has a different reference. It happens to be simple enough to convert to tunnel coordinates. If only the PIV coordinates are negated they coincide with the coordinates of the figure above.

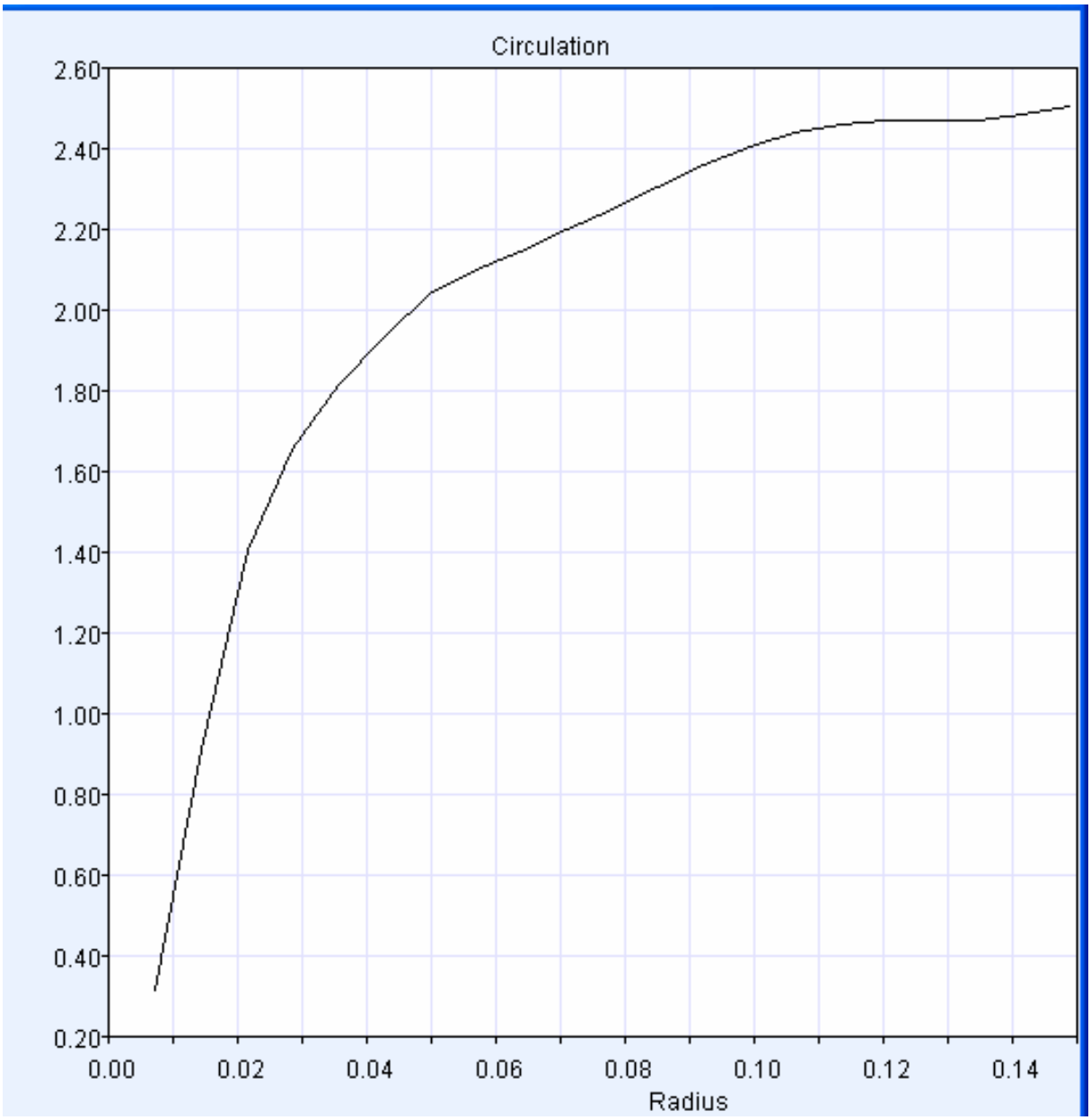

The expected behavior of the curve reflects the idea of asymptotic behavior. However, the approach to a final level does not seem to have matured distinctively when the curve is cut off by the edge of the PIV sheet. After many similar studies it can be stated that the attainment of a convincing asymptote escapes the analyst. A disturbance to a possible increase of the PIV sheet would allow a greater radius. But, then the integration circle will eventually infringe upon the next vortex with a confusing increase in the curve. It can be speculated that the part of the curve forming a plateau is the asymptotic level and the last uphill behavior reflects the capture of infinitesimal fibers from the next (or neighboring) vortex/vortices. This thought will, for a while, remain among unsupported ideas until further evidence from the database can be retrieved.

One computer method allowed the PIV sheet to be traversed along a straight track intersecting the vortex center. The track, which was represented by 50 points in the computer code, thus carries the information of three speed vector components for each of the 50 points. Consequently the u component can be plotted separately as a function of x if the track is oriented mainly in the x direction otherwise y was chosen as the independent variable. Similarly the other two components v and w were plotted. In the following group of diagrams there is also a fourth characterized as uv vs independent coordinate. uv is the absolute velocity in the PIV plane, i.e. the vector sum of u and v.

The diagrams below are the result of the cross-PIV-track technique.

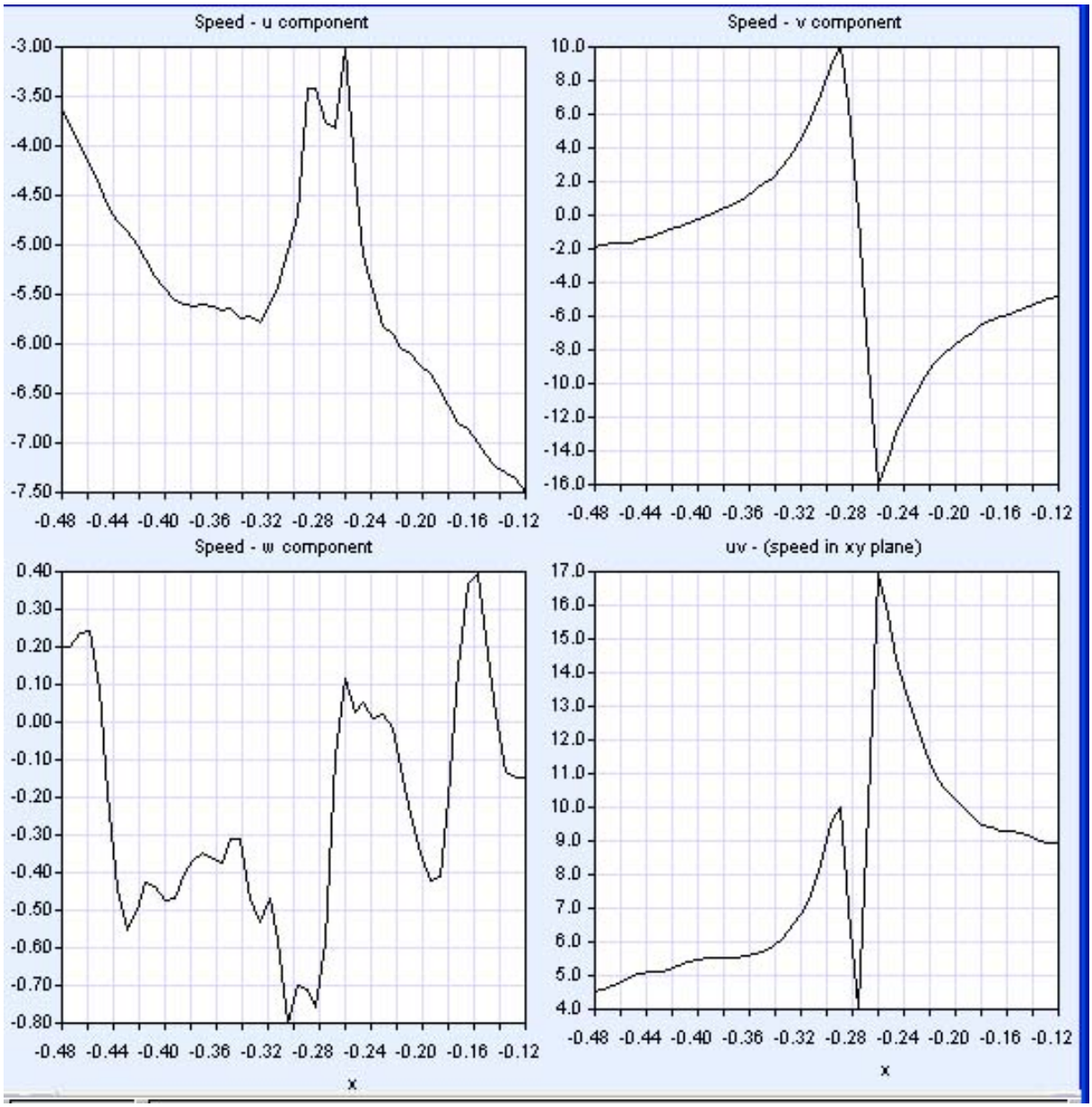

The u component includes the wind tunnel speed of 10 m/s + the disturbance from deceleration through the rotor + the influence from the vortex. Its validity as a base for quick learning can therefore be left aside. It is too complicated.

The v component, however, is relatively unperturbed since it is vertical and the tunnel speed is essentially oriented x-wise. The diagram amazingly portrays a schoolbook picture of the speed cross section of a real vortex. The core is seen to be 3 cm in diameter. The difference in speed between max and min is 6m/s. This means that the maximum vortex rotation speed of 6/2=3 m/s occurs at a radius of 1.5 cm from the center.

An observation that can be made is that the v component asymptotic behaviors to the right and to the left are truncated by the limitation of the PIV sheet. If the vortex were two-dimensional the left and the right flanks would eventually converge toward the same level. The reason is that the flow, in this particular region of the test section, is very actively changing its speed and direction. The flow lines are bent and the x direction chosen for the cross-PIV path goes from outside the wake to the inside.

Groping for solutions to unanswered questions it is tempting to speculate at what level the circulation would assume asymptotic value. A mathematical curve fit equation could easily be constructed to emulate the v component behavior. The point of symmetry would be chosen midway between the top value and the bottom value. In the next step the circulation would be evaluated analytically from the curve fit equation. This path of venture remains to be explored for the future.

The graphs are based on an average of many PIV sheets in the same position with the same trigger conditions. The average PIV sheet gives smoother cross-PIV curves than those of the individual cases – as should be expected. Several individual cases, although displaying intense jitter in the cross-PIV curves resulted in circulation curves, which were surprisingly similar to the one presented above. Part of the explanation is that it is in the nature of integration to smoothen ripples in a curve. Thus speed is rough and circulation is smooth.

The circulation reaching a value of say 2.5, according to the circulation diagram, should also reflect the level of the maximum circulation on the blade. But, does it? – The question is answered in the next section.

3.2 Bound circulation

The circulation bound to the blade is connected with lift and loading as follows. A relationship can be found by equating two expressions for lift as follows.

$$dL = q_L C_L dS = \frac{1}{2}\rho V_L^2 \cdot C_L c \cdot dr = \Gamma \rho V_L dr \quad (2)$$

where

$$V_L = \sqrt{\left(u(1-a)\right)^2 + \left(\omega r(1+a')\right)^2} \quad (3)$$

$$\Gamma = \frac{1}{2} V_L c C_L(\alpha) \quad (4)$$

where

$\rho =$ Density of air

$V_L =$ Local velocity at radius r

$C_L =$ Local lift coefficient

$c =$ Local chord length

$dr =$ Radial extent of a small area around the radial point of evaluation

Γ is called the bound circulation.

From the Mexico data the normal coefficient *Cn* and the tangential coefficient *Ct* are available for the 5 stations along the blade in the 100 GB database. *Cn* and *Ct* represent forces, which are perpendicular and aligned with the profile chord line at the local radial station. The vector sum of the two becomes the aerodynamic force coefficient. The same approach can be taken with respect to the wind aligned coefficients C_L and C_D. The angular difference between the force represented by C_L and that represented by *Cn* is the angle of attack α. From simple geometrical considerations the following relations are so derived.

$$C_L = \cos\alpha \cdot C_n - \sin\alpha \cdot C_t \quad (4)$$

$$C_D = \sin\alpha \cdot C_n + \cos\alpha \cdot C_t \quad (5)$$

The coefficients *Cn* and *Ct*, based on the pressure recordings from the measurements, lack the influence of aerodynamic friction. Approximations were considered but abandoned after finding other sources of uncertainly. It should be noted that Ct is defined positive pointing backward toward the trailing edge. It normally is numerically negative.

Obviously the angle of attack is required to calculate C_L such that Γ can be calculated according to Eq. (4). An approximation for the angle of attack is obtained from the speed triangle at a close-up view of the section of the blade at radius r.

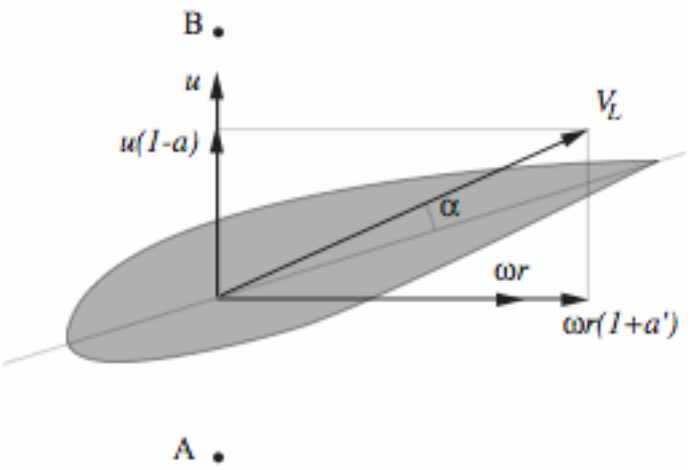

Basic 2D view of profile for calculation of angle of attack

The effective local velocity, forming the angle of attack with the chord line, is seen to be obtainable using the Pythagorean theorem. The PIV measurements provide speed information in arbitrary points, within a PIV sheet. The figure shows two points A and B approximately chosen such that the *u* components in these points can be used to evaluate the arithmetic average as the representative value of $u(1-a)$. If the curvy flow lines are imagined around the profile it is immediately clear that the profile disturbance influence poses difficulties to trust the u components in A and B. One way to avoid this curviness is to increase the distance between A and B. But then the interpolation can no longer be trusted to be linear.

For this preliminary analysis there was no time to develop these thoughts. Instead equations were developed based on the figure above and estimates of *a* were used. It turns out that the result in C_L is relatively insensitive to errors in *a*. The tangential induction *a´* is obtained by assuming that the induced velocity vector, i.e. (ωr *a´*, -*au*), is perpendicular to the resulting local velocity V_L. This gives

$$\alpha = a\tan\frac{(1-a)V_\infty}{\omega r(1+a')} - \varphi \qquad (6)$$

φ is the local twist+pitch angle. For *a´* the following expression can be derived

$$a' = \frac{1}{2}\sqrt{1+\frac{4a(1-a)}{(\lambda x)^2}} - 1 \qquad (7)$$

where

λ = Tip speed ratio

$x = r/R$

These equations were applied to find the bound circulation. The radial pressure distribution extraction was repeated for 6 azimuth angles during the testing. When the azimuth angle for blade 1 was 180 degrees the two outermost pressure stations, at 82 and 92%, were seen to deviate from the pattern. Therefore 180 degrees was discarded when an average over azimuth was calculated and used to derive *Cn* and *Ct*.

It turned out that the station at 82% of tip radius had the highest value of circulation along the radius. The coherent numbers arrived at were as follows.

Radius at 82% = 1.845
Assumed a = 0.3
Vinf = 10 m/s
Chord = 0.116
Twist+pitch = +0.3
Cn = 0.5338
Ct = -0.0176
$\alpha = 4.13°$
CL = 0.5337
Γ = 2.56 (circulation)

It is surprising how well this circulation value agrees with that in the free tip vortex, see the Γ vs radius diagram above. But, more evaluations for different cases are needed to assess with certainty how well the two values can be expected to agree.

3.2 Speed Information from the Tunnel Reference System and PIV – a Comparison
One sequence of measurements was set up such that the tunnel flow would be mapped from well ahead to well behind the turbine. The extent of the PIV sheet placements can be appreciated from the figure below.

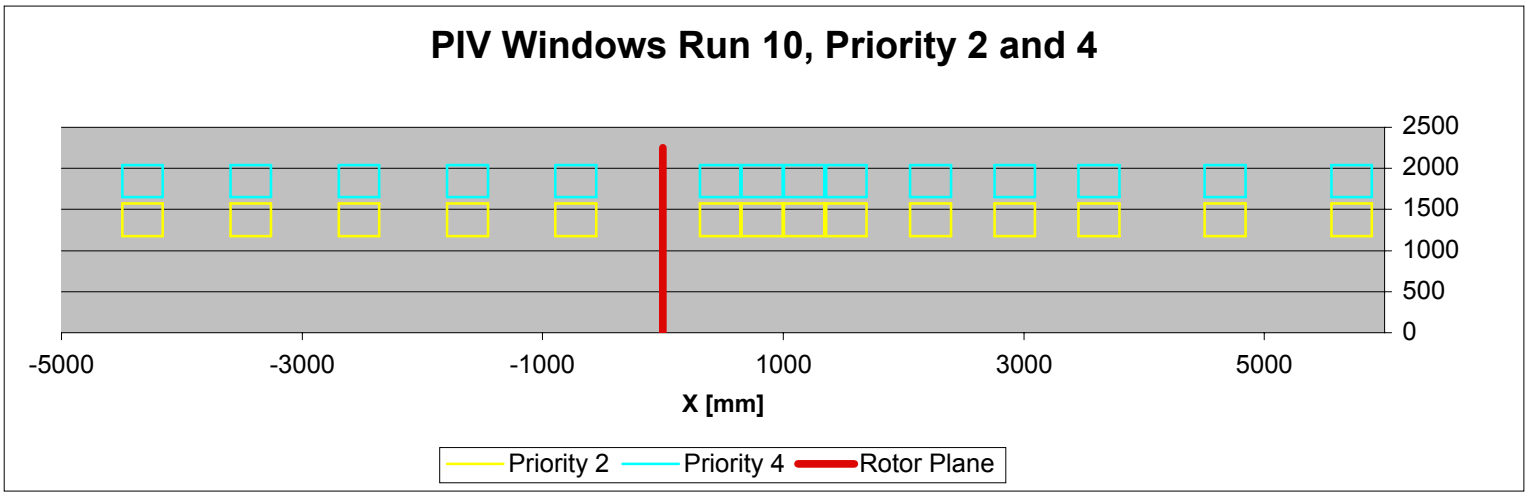

The lower sequence (at the lower radius), in the preceding figure, was used for extraction of the following figure, which depicts the average u component velocity as averaged over each PIV sheet.

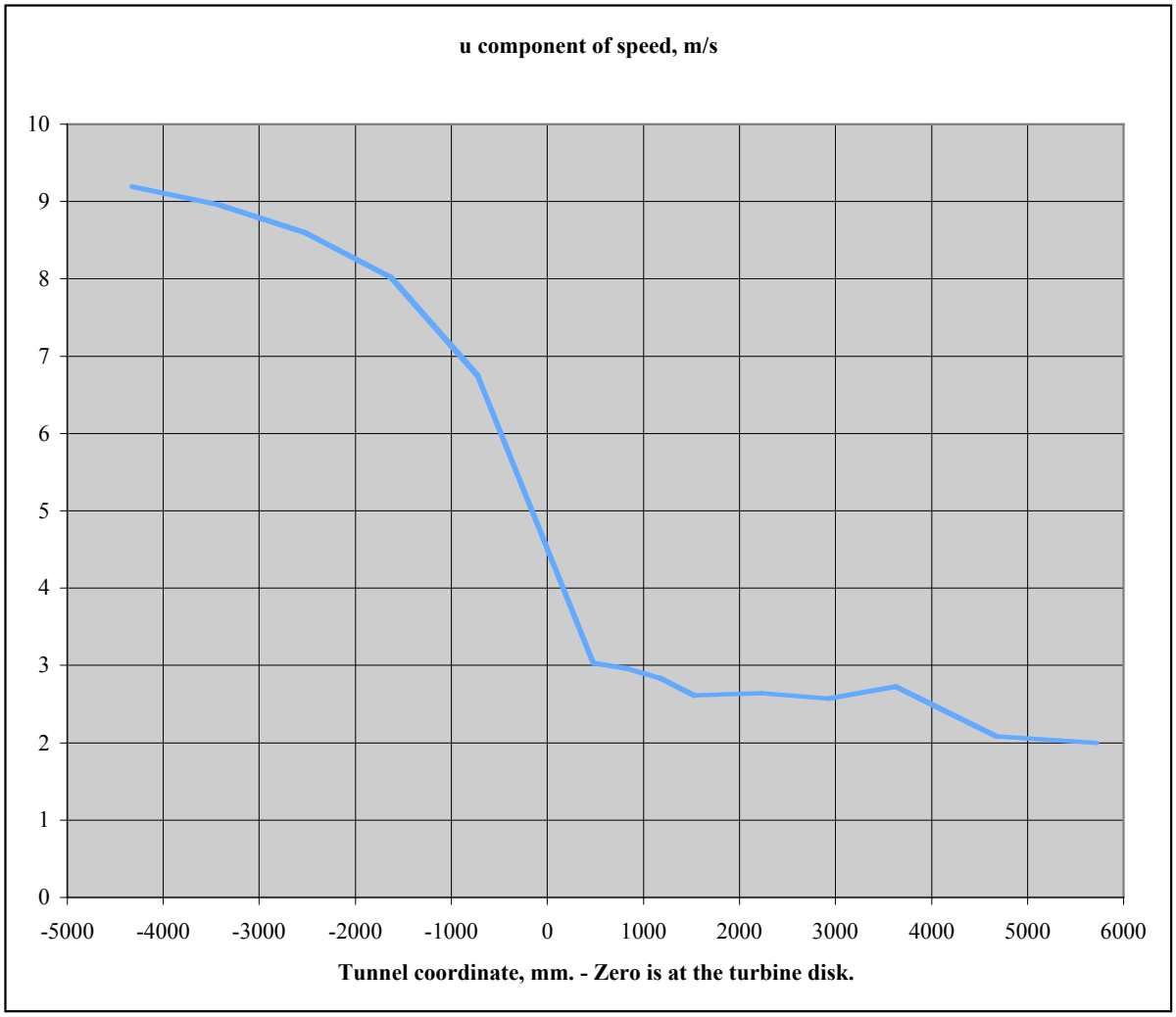

The case chosen is to be considered “difficult” in the sense that the deceleration of the flow is considerable. In the wake especially the variation from one PIV sheet to the next, for the same location, is highly variable. This reveals a turbulent wake, which is far from steady. (A large number of PIV sheets exist for each location.)

It may come as a surprise that the apparent deceleration starts so early, in fact one diameter upstream of the turbine. Another surprise is that the leftmost point on the curve is not higher. The nominal tunnel speed was 10 m/s.

Because of the open jet section it was established as a fact that the flow before and especially inside the collector would be accelerated in order for the condition of continuity of the flow to be heeded. Although the major acceleration can be expected to take place outside the wake, not even a slight tendency of the wake flow is seen to accelerate. The curve in fact shows the opposite. At the moment there is no other explanation available than to refer to the high level of turbulence in the wake, which disturbs the average. The figures were derived from individual PIV sheets rather than from the average from each position. It will be a desirable feature of a future investigation to include a study using the average information in this context.

Appendix B: Analysis of PIV data (Provided by Herman Snel from ECN)

The PIV traverses in flow direction, from approximately 1 rotor diameter upwind to approximately 1.25 rotor diameters downwind of the rotor plane, permit a very good appraisal of the development of the induction field of the rotor. As a first check, the axial velocity component was determined for the case of zero yaw, 100 m/s tip speed and 15 m/s tunnel speed. For this case, the tip speed ratio (6.7) equals the design tip speed ratio. The results are shown in the figure below for the two radial positions that formed the centre of the PIV sheets used in the traverses, 61% and 82% of the radius respectively. In the graph a theoretical curve is also shown, as resulting from a cylindrical wake model

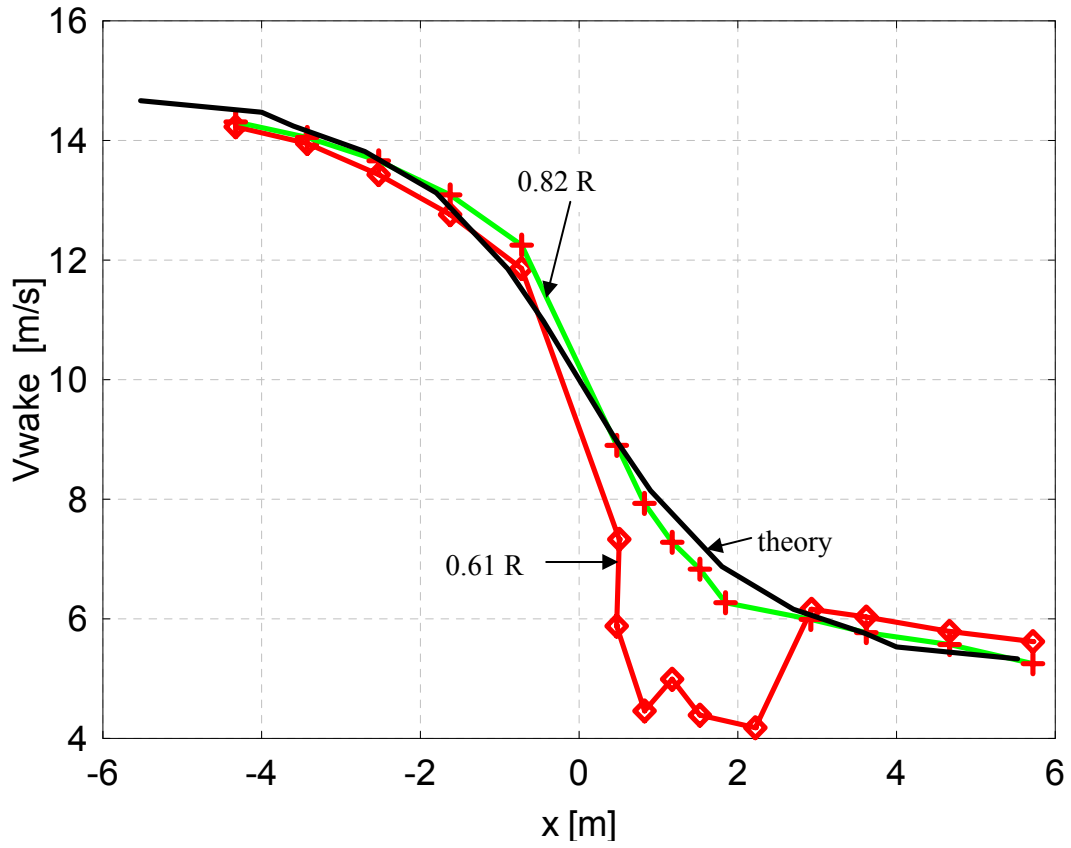

It is observed that the 82% traverse shows good agreement with the simplified theory both upstream and downstream. The 61% shows good agreement upstream but a very different behaviour directly downstream of the rotor. Inspection of the corresponding PIV sheet directly downstream shows the release of a trailing vortical structure at this position, undoubtedly linked to the induction behaviour. This phenomenon will constitute a very serious verification case for both CFD codes and free vortex wake codes. Once completely understood, it can be used to modify BEM in regions where large gradients occur of the bound vorticity on the blade. It is noted that the induction at the rotor plane position is very close to 1/3 as should be expected for the design tip speed ratio.

For the same case, the approximate tip vortex trajectory was obtained from the PIV sheets following the vortex positions. This also allowed an estimation of the vortex transport velocity, allowing the future verification of free vortex models and the construction of prescribed vortex wake models. The results are shown in the figure below:

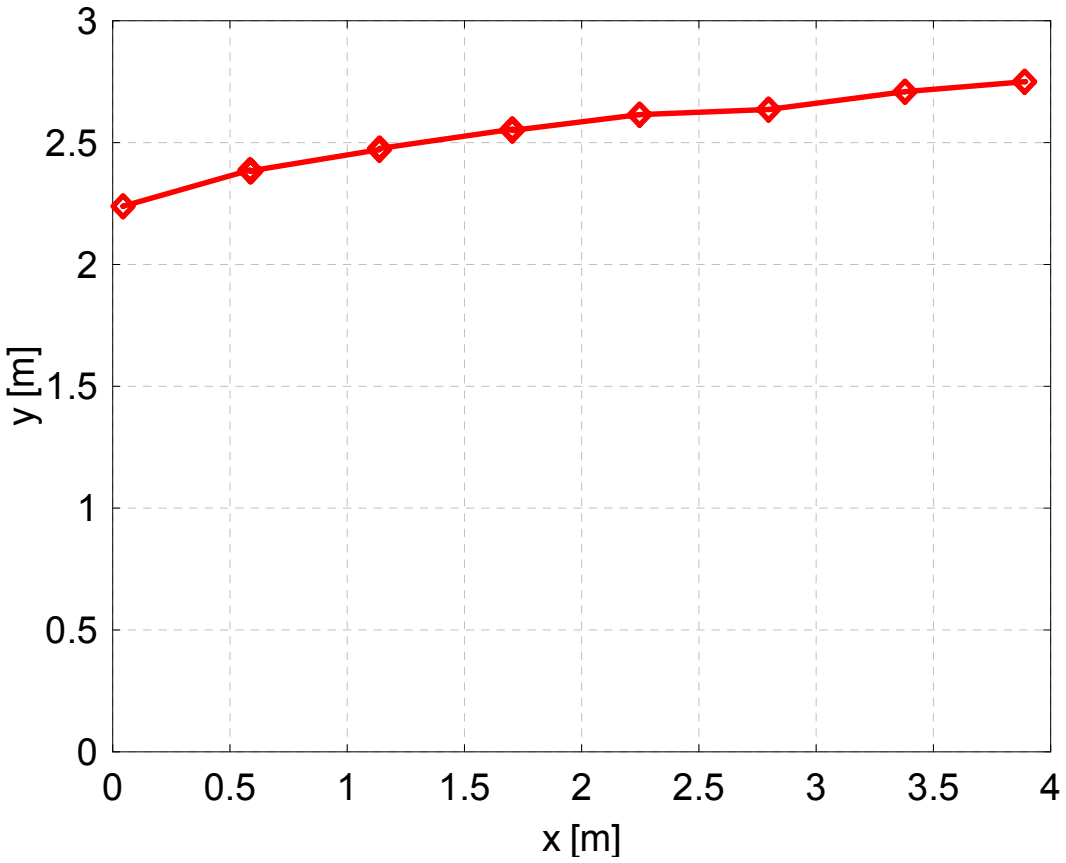

The approximate travel speed is shown in the table below:

Vortices	distance	Travel speed
1-2	0.544	11.55
2-3	0.55	11.68
3-4	0.566	12.02
4-5	0.543	11.53
5-6	0.55	11.68
6-7	0.582	12.36
7-8	0.51	11.46

Notice that, the transport speed does not seem to decrease with distance. This is contrary to some intuitive models that assume the transport speed to be the average of the wake speed and the undisturbed outer speed.
The tip vortex intersection with the PIV plane was clearly determinable up to the last PIV position that could be used for vortex tracking, about one diameter behind the rotor. Note at this eighth vortex intersection, it is the third time that the vortex trailed from blade 3 passes through the horizontal plane in which all PIV sheets are located.

A clear picture of the flow structure in the direct neighborhood of a vortex is shown in the figure below, in which horizontal projections of the streamlines are shown. The vortex position shown is the second position of the previous figure, at approximately 0.12 D behind the rotor.

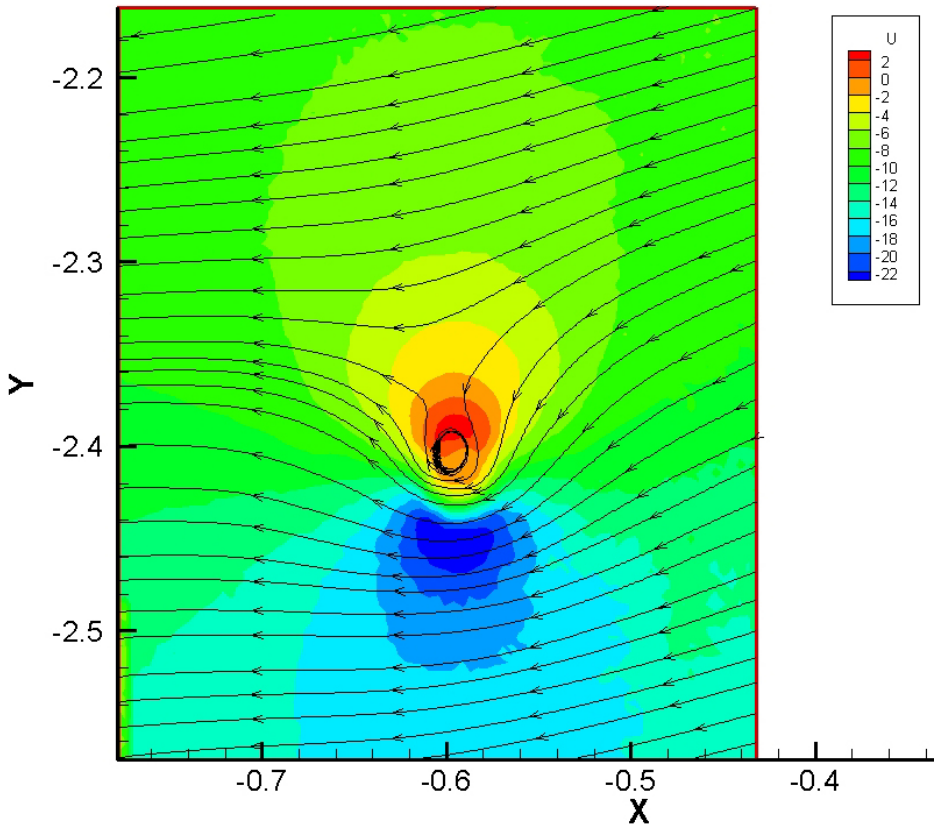

The colors in the graph map the values of the axial velocity component. Its values are close to 15 m/s in the bottom of the graph (outer flow) and about 10 m/s in the top part (wake flow)

Further, to check the detail of information present in the PIV sheets, some of the sheets taken in the rotor plane were inspected. This was done for the case of 30 degrees yaw misalignment. The following figure shows a representation of the velocity field, with the average value of the velocity components subtracted. This PIV shot was taken 10 degrees (i.e $1/36^{th}$ of a revolution) after rotor blade passing. The green line that crosses the sheet shows upflow, normal to the sheet, at a small downstream distance of where the blade passed. This region is the velocity deficit of the viscous wake. Pictures of this type are a testimony to the great flow detail present in the PIV measurements, which will be used for a very precise description of the flow field. PIV shots like this where taken at 20 degrees interval of rotor azimuth position, allowing the determination of induction in position between blades. Towards the tip, this will be used to refine tip correction models, also for yawed flow. Both for axial and yawed flow, this type of information was not available from measurements previously.

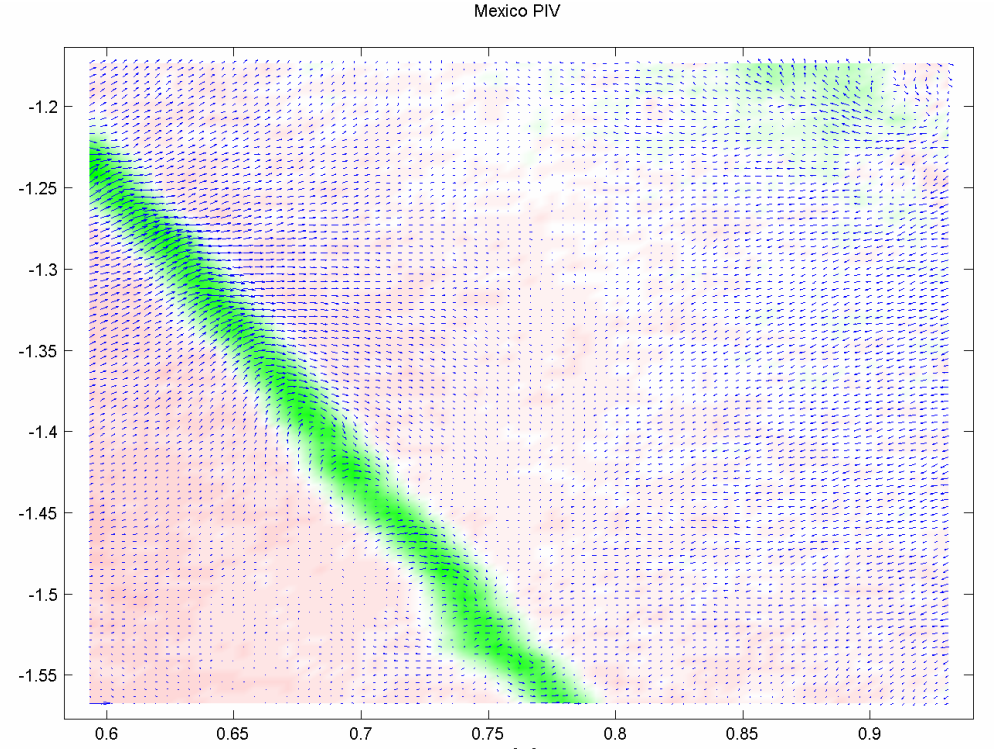

The flow is from right to left, the blade tip is below the bottom of the graph

Appendix C: Budgets

		Budget	Actual budget spent (kEur)						Total	Total(accumulated) budget spent (%)						Remaining budget (kEur)
			Year 1	Year 2	Year 3	Year 4	Year 5	Year 6		Year 1	Year 2	Year 3	Year 4	Year 5	Year 6	
ECN	Labour	185849	51000	67200	65955	22533	12019	35793	254500	0.27442	0.636	0.99089	1.11213	1.1768	1.3694	-68651
	Overhead	108412	31000	40800	40400	13680	7286	21692	154858	0.28595	0.66229	1.03494	1.16113	1.22833	1.42844	-46446
	Pers. Costs	294261	82000	108000	106355	36213	19305	57485	409358	0.27866	0.64569	1.00712	1.13018	1.19579	1.39115	-115097
	Travel	15000	6500	0.6	4000	70	0.3	1000	11570.9	0.43333	0.43337	0.70004	0.70471	0.70473	0.77144	3429.1
	Durable equipment								0							0
	Consumables								0							0
	External assistance	83000			18300			54300	72600	0	0	0.22048	0.22048	0.22048	0.8747	10400
	Others		2600		1750				4350							-4350
	TOTAL	392261	91100	108000.6	130405	36283	19305	112785	497879	0.23224	0.50757	0.84002	0.93251	0.98173	1.26926	-105618
NLR	Labour	57035	15904	15876	8901	279	5502	46493	92955.1	0.27885	0.5572	0.71327	0.71816	0.81462	1.6298	-35920
	Overhead	102648	29424	25561	15577	527	11003	44168	126260	0.28665	0.53567	0.68742	0.69255	0.79974	1.23004	-23612
	Pers. Costs	159683	45328	41437	24479	805	16505	90661	219215	0.28386	0.54336	0.69665	0.7017	0.80506	1.37282	-59532
	Travel	9000	3154	171	1039			240	4604.44	0.35044	0.36944	0.48494	0.48494	0.48494	0.51166	4395.56
	Durable equipment								0							0
	Consumables			18	143	20	261	247	688.64							-688.64
	External assistance	38000	1924					38000	39924	0.05063	0.05063	0.05063	0.05063	0.05063	1.05063	-1924
	Others	8000	45					1874	1919	0.00563	0.00563	0.00563	0.00563	0.00563	0.23988	6081
	TOTAL	214683	50451	41626	25661	825.25	16766	131022	266351	0.235	0.4289	0.54843	0.55227	0.63037	1.24068	-51668
DUT	Labour	53857	15150	17208	25114.9	13207	19364		90043.9	0.2813	0.60081	1.06714	1.31236	1.67191	1.67194	-36187
	Overhead	30885	8686	9864	15522.7	8430	14523		57025.7	0.28124	0.60062	1.10321	1.37616	1.84639	1.84645	-26141
	Pers. Costs	84742	23836	27072	40637.5	21637	33887		147070	0.28128	0.60074	1.08029	1.33561	1.7355	1.73552	-62328
	Travel	9000	4080	2333	1992.6	129.82	150		8685.42	0.45333	0.71256	0.93396	0.94838	0.96505	0.96515	314.58
	Durable equipment					0			0							0
	Consumables	75231	214	6517	494	0	34210		41435	0.00284	0.08947	0.09604	0.09604	0.55077	0.55078	33796
	External assistance	97500				35000	0	52000	87000	0	0	0	0.35897	0.35897	0.89231	10500
	Others	78000		96999		0	0		96999	0	1.24358	1.24358	1.24358	1.24358	1.24359	-18999
	TOTAL	344473	28130	132921	43124.1	56766.8	68247	52000	381189	0.08166	0.46753	0.59272	0.75751	0.95563	1.10659	-36716
Polymari	Labour		3300						3300							
	Overhead		1300						1300							
	Pers. Costs		4600						4600							
	Travel		600						600							
	Durable equipment								0							
	Consumables								0							
	External assistance								0							
	Others								0							
	TOTAL	28000	9800			0	0	0	9800						0.35	
Technion	Labour	22370	12034	10335.99	0	0	0	0	22370	0.53795	1	1	1	1	1.00004	0.01
	Overhead	76434	3904	26247.50	55712			0	85863.5	0.05108	0.39448	1.12337	1.12337	1.12337	1.12338	-9429.5
	Pers. Costs	98804	15938	36583.49	55712		0		108233	0.16131	0.53157	1.09544	1.09544	1.09544	1.09545	-9429.5
	Travel	15000	5338		5717.57			4773	15828.6	0.35587	0.35587	0.73704	0.73704	0.73704	1.05529	-828.57
	Durable equipment				0				0							0
	Consumables	41590			41590	14		4802	46406						1.1158	-4816
	External assistance	26000			0	48400	106000	85064	239464	0	0	0	1.86154	5.93846	9.21038	-213464
	Others	303209	2150	120901.93	231250	239000	44800		638102	0.00709	0.40583	1.16851	1.95674	2.1045	2.1045	-334893
	TOTAL	484603	23426	157485.42	334270	287414	150800	94639	1048034	0.04834	0.37332	1.0631	1.65619	1.96737	2.16267	-563431
Risoe	Labour	98843	49497	29378	8693	9410	0	14863	111841	0.50076	0.79798	0.88593	0.98113	0.98113	1.13151	-12998
	Overhead	108744	54446	30847	9127	9881	0	15595	119896	0.50068	0.78435	0.86828	0.95914	0.95914	1.10256	-11152
	Pers. Costs	207587	103943	60225	17820	19291	0	30458	231737	0.50072	0.79084	0.87668	0.96961	0.96961	1.11634	-24150
	Travel	11000	2964	1931	1403			2125	8423	0.26945	0.445	0.57255	0.57255	0.57255	0.76578	2577
	Durable equipment								0							0
	Consumables		1134	0				1583	2717							-2717
	External assistance	50000						48438	48438	0	0	0	0	0	0.96876	1562
	Others								0							0
	TOTAL	268587	108041	62156	19223	19291	0	82604	291315	0.40226	0.63368	0.70525	0.77707	0.77707	1.08462	-22728

		Budget	Actual budget spent (kEur)						Total	Total(accumulated) budget spent (%)						Remaining budget (kEur)
			Year 1	Year 2	Year 3	Year 4	Year 5			Year 1	Year 2	Year 3	Year 4	Year 5	Year 6	
DTU	Labour	69101	10629	15945	25804	3700	13023		69101	0.15382	0.38457	0.75799	0.81154	1	1.00001	0
	Overhead	16210	2711	3589	5161	740	2605		14806	0.16724	0.38865	0.70703	0.75268	0.91339	0.91344	1404
	Pers. Costs	85311	13340	19534	30965	4440	15628		83907	0.15637	0.38534	0.74831	0.80035	0.98354	0.98355	1404
	Travel	9000	1928	1003	788				3719	0.21422	0.32567	0.41322	0.41322	0.41322	0.41327	5281
	Durable equipment								0							0
	Consumables								0							0
	External assistance	19000						19000	19000	0	0	0	0	0	1	0
	Others	3000	1000	1000			1000		3000	0.33333	0.66667	0.66667	0.66667	1	1.00033	0
	TOTAL	116311	16268	21537	31753	4440	16628	19000	109626	0.13987	0.32503	0.59803	0.63621	0.77917	0.94253	6685
FOI	Labour	61869	18236.6	12890.2	5992	572.4	140.27	1372.9	39204.4	0.29476	0.50311	0.59996	0.60921	0.61148	0.63368	22664.6
	Overhead	22561	14860	13197.1	7561	738.7	175.34	1144.1	37676.2	0.65866	1.24361	1.57875	1.61149	1.61926	1.67004	-15115
	Pers. Costs	84430	33096.6	26087.3	13553	1311.1	315.61	2517	76880.6	0.392	0.70098	0.86151	0.87703	0.88077	0.91059	7549.39
	Travel	9000	1859.9	1030.7	114		0		3004.6	0.20666	0.32118	0.33384	0.33384	0.33384	0.33388	5995.4
	Durable equipment								0							0
	Consumables	5000							0	0	0	0	0	0	0	5000
	External assistance	20000						19984	19983.9	0	0	0	0	0	0.9992	16.1
	Others	0						14067	14066.5							-14067
	TOTAL	118430	34956.5	27118	13667	1311.1	315.61	36567	113936	0.29517	0.52415	0.63955	0.65062	0.65328	0.96206	4494.39
CRES	Labour	52387	32748	15078	2974	0		2319	53119	0.62512	0.91294	0.96971	0.96971	0.96971	1.01399	-732
	Overhead	52387	29473	14324	2825	0		2087	48709	0.5626	0.83603	0.88995	0.88995	0.88995	0.92981	3678
	Pers. Costs	104774	62221	29402	5799	0	0	4406	101828	0.59386	0.87448	0.92983	0.92983	0.92983	0.97189	2946
	Travel	9000	4620	1176	2467	0		2001.8	10264.8	0.51333	0.644	0.91811	0.91811	0.91811	1.14064	-1264.8
	Durable equipment								0							0
	Consumables								0							0
	External assistance	20000						20000	20000	0	0	0			1	0
	Others	0	493						493							-493
	TOTAL	133774	67334	30578	8266	0	0	26408	132586	0.50334	0.73192	0.79371	0.79371	0.79371	0.99112	1188.2
NTUA	Labour	40270	20664	9415		0		2240	32319	0.51314	0.74693	0.74693	0.74693	0.74693	0.80258	7951
	Overhead	33434	6003	2822.8	269.06	0.00	16812	448	26354.9	0.17955	0.26398	0.27202	0.27202	0.77487	0.78829	7079.14
	Pers. Costs	73704	26667	12237.8	269.06	0	16812	2688	58673.9	0.36181	0.52785	0.5315	0.5315	0.7596	0.79608	15030.1
	Travel	9000	4350	1199	1345.3				6894.28	0.48333	0.61656	0.76603	0.76603	0.76603	0.76612	2105.72
	Durable equipment								0							0
	Consumables								0							0
	External assistance	18000		0				43710	43710	0	0	0	0	0	2.42833	-25710
	Others	117900	5000	3500			84059		92559.4	0.04241	0.07209	0.07209	0.07209	0.78507	0.78507	25340.6
	TOTAL	218604	36017	16936.8	1883.4	0	100871	46398	201838	0.16476	0.24224	0.25085	0.25085	0.71229	0.92454	16766.4

APPENDIX D: OVERVIEW OF MANHOURS SPENT

Task	Partner	Planned effort (mm)						Total	Actual effort						Total	Deviation
		Year 1	Year 2	Year 3	Year 4	Year 5	Year 6		Year 1	Year 2	Year 3	Year 4	Year 5	Year 6		
1. Baseline def.	ECN	2.8						2.8	0.78	0.22					1	-1.8
	NLR	0.3						0.3	0.3						0.3	0
	DUT	0.24						0.24	0.25						0.25	0.01
	Technior	0						0	2	1					3	3
	RISOE	0.6						0.6	1						1	0.4
	DTU	0.5						0.5	0.5						0.5	0
	FFA	0.5						0.5	0.5						0.5	0
	CRES	0.3						0.3	2.22						2.22	1.92
	NTUA	0.5						0.5	0.5						0.5	0
TOTAL		5.74	0	0	0		0	5.74	8.05	1.22	0	0	0	0	9.27	3.53
2. NS + E simulatio	ECN			0.5				0.5			1.3				1.3	0.8
	NLR			1				1	0.3		0.4				0.7	-0.3
	DUT							0							0	0
	Technion							0							0	0
	RISOE	2		2	2		1.5	7.5	3.5					1	4.5	-3
	DTU	1.5	2					3.5	1.5	2	2				5.5	2
	FFA							0							0	0
	CRES	1		1	2		1	5	2.2		1			2	5.2	0.2
	NTUA	3						3	3						3	0
TOTAL		7.5	2	4.5	4		2.5	20.5	10.5	2	4.7	0	0	3	20.2	-0.3
3 Aero rotor design	ECN	1						1	0.75						0.75	-0.25
	NLR							0							0	0
	DUT	0.5	2	1.75				4.25	0.25	0.25	1				1.5	-2.75
	Technior	1.1	0.4					1.5	0.6	0.9	4				5.5	4
	RISOE	0.5						0.5	0.5						0.5	0
	DTU							0							0	0
	FFA							0							0	0
	CRES	4						4	4						4	0
	NTUA							0							0	0
TOTAL		7.1	2.4	1.75	0		0	11.25	6.1	1.15	5	0	0	0	12.25	1
4. Struct. Rotor des	ECN	0.25	0.25	0.7				1.2	0.25	0.25	0.5	0.5			1.5	0.3
	NLR							0							0	0
	DUT							0							0	0
	Technion							0			2				2	2
	RISOE							0							0	0
	DTU							0							0	0
	FFA							0							0	0
	CRES							0							0	0
	NTUA							0							0	0
TOTAL		0.25	0.25	0.7	0		0	1.2	0.25	0.25	2.5	0.5	0	0	3.5	2.3
5. Design of DAS	ECN	1						1		1					1	0
	NLR	5.25			0			5.25	2.06	2.79	0.87				5.72	0.47
	DUT	1	1	0.25				2.25	1.5	0.5	0.5	0.5			3	0.75
	Technion							0							0	0
	RISOE							0							0	0
	DTU							0							0	0
	FFA							0							0	0
	CRES							0							0	0
	NTUA							0							0	0
TOTAL		7.25	1	0.25	0		0	8.5	3.56	4.29	1.37	0.5	0	0	9.72	1.22
6. Model constructi	ECN	0.25	0.25					0.5	0.09	0.41				0.6	1.1	0.6
	NLR	0.25	0.25					0.5	0.3	0.2	0.33			3.46	4.29	3.79
	DUT							0							0	0
	Technior	0	3.5	3.5	0.5			7.5	0	3.5	32				35.5	28
	RISOE							0							0	0
	DTU							0							0	0
	FFA							0							0	0
	CRES							0							0	0
	NTUA	0.5	0.5					1	0.5						0.5	-0.5
TOTAL		1	4.5	3.5	0.5		0	9.5	0.89	4.11	32.33	0	0	4.06	41.39	31.89
7. Exp matrix defini	ECN	0.5			0.1			0.6	0.02	0.48					0.5	-0.1
	NLR	0.5			0.2			0.7	0.4		0.1	0.05	0.42		0.97	0.27
	DUT	0.25			0.25			0.5	0.25						0.25	-0.25
	Technion		1					1		1					1	0
	RISOE	2.5			1			3.5	3			1		1	5	1.5
	DTU				0.5			0.5							0	-0.5
	FFA	0.5	1		0.5			2	1	1	0.1				2.1	0.1
	CRES	0.5						0.5	2.22						2.22	1.72
	NTUA	0.25						0.25	0.25						0.25	0
TOTAL		5	2	0	2.55		0	9.55	7.14	2.48	0.2	1.05	0.42	1	12.29	2.74

Task	Partner	Planned effort (mm)						Total	Actual effort						Total	Deviation
		Year 1	Year 2	Year 3	Year 4	Year 5	Year 6		Year 1	Year 2	Year 3	Year 4	Year 5	Year 6		
8. Flow viz. Prepara	ECN	1	0.5					1.5	0.14	1.36					1.5	0
	NLR	0.125	0.125					0.25	0.2	0.05					0.25	0
	DUT	0.2	0.4					0.6	0.2	0.4					0.6	0
	Technion							0							0	0
	RISOE							0							0	0
	DTU							0							0	0
	FFA	0.5	1	0.5				2	1	0.9	0.1				2	0
	CRES							0							0	0
	NTUA							0							0	0
TOTAL		1.825	2.025	0.5	0		0	4.35	1.54	2.71	0.1	0	0	0	4.35	0
9. Meas. Probe cali	ECN							0							0	0
	NLR							0							0	0
	DUT	0.1	0.1					0.2	0.1	0.1					0.2	0
	Technion							0							0	0
	RISOE							0							0	0
	DTU							0							0	0
	FFA							0							0	0
	CRES							0							0	0
	NTUA							0							0	0
TOTAL		0.1	0.1	0	0		0	0.2	0.1	0.1	0	0	0	0	0.2	0
10. 2D profile meas	ECN							0							0	0
	NLR							0							0	0
	DUT		1	1.5	1			3.5	0.5	0.5	2.5	1.75	4		9.25	5.75
	Technion							0							0	0
	RISOE							0							0	0
	DTU							0							0	0
	FFA							0							0	0
	CRES							0							0	0
	NTUA							0							0	0
TOTAL		0	1	1.5	1		0	3.5	0.5	0.5	2.5	1.75	4	0	9.25	5.75
11. Measurements	ECN						1	1						1.5	1.5	0.5
	NLR				0		4.5	4.5						3	3	-1.5
	DUT						0.5	0.5							0	-0.5
	Technion							0							0	0
	RISOE							0							0	0
	DTU							0							0	0
	FFA						1	1							0	-1
	CRES							0							0	0
	NTUA							0							0	0
TOTAL		0	0	0	0		7	7	0	0	0	0	0	4.5	4.5	-2.5
12. Data proc. and	ECN						1.5	1.5							0	-1.5
	NLR						3.2	3.2					0.3	1.21	1.51	-1.69
	DUT						0.75	0.75	0.25	0.5					0.75	0
	Technion						1.3	1.3							0	-1.3
	RISOE						1	1							0	-1
	DTU						1	1		0.5	0.5				1	0
	FFA						1.3	1.3							0	-1.3
	CRES	1					1.5	2.5		1					1	-1.5
	NTUA							0							0	0
TOTAL		1	0	0			11.55	12.55	0.25	2	0.5	0	0.3	1.21	4.26	-8.29
13. Data archiving	ECN						1.5	1.5							0	-1.5
	NLR						0	0							0	0
	DUT							0							0	0
	Technion							0							0	0
	RISOE							0							0	0
	DTU							0							0	0
	FFA							0							0	0
	CRES							0							0	0
	NTUA							0							0	0
TOTAL		0	0	0			1.5	1.5	0	0	0	0	0	0	0	-1.5
14. BEM adaptatior	ECN						2.5	2.5							0	-2.5
	NLR							0							0	0
	DUT						1	1							0	-1
	Technion						3.5	3.5							0	-3.5
	RISOE						3	3							0	-3
	DTU						6	6			3	1		2	6	0
	FFA						2	2							0	-2
	CRES						4	4							0	-4
	NTUA						0	0							0	0
TOTAL				0			22	22	0	0	3	1	0	2	6	-16

Task	Partner	Planned effort (mm)						Total	Actual effort						Total	Deviation
		Year 1	Year 2	Year 3	Year 4	Year 5	Year 6		Year 1	Year 2	Year 3	Year 4	Year 5	Year 6		
15. Rules for blm's	ECN						1	1							0	-1
	NLR							0							0	0
	DUT						0.5	0.5							0	-0.5
	Technion							0							0	0
	RISOE						1	1							0	-1
	DTU							0							0	0
	FFA							0							0	0
	CRES						1.5	1.5						2	2	0.5
	NTUA							0							0	0
TOTAL				0			4	4	0	0	0	0	0	2	2	-2
16. NS validation	ECN							0							0	0
	NLR							0							0	0
	DUT							0							0	0
	Technion							0							0	0
	RISOE			1	1		2	4			1	0.44			1.44	-2.56
	DTU			2.5				2.5			2.5				2.5	0
	FFA							0							0	0
	CRES				1.75		3.75	5.5						5	5	-0.5
	NTUA	1	2				1.25	4.25	1	2					3	-1.25
TOTAL		1	2	3.5	2.75		7	16.25	1	2	3.5	0.44	0	5	11.94	-4.31
17. Reporting and c	ECN						2	2							0	-2
	NLR			0				0							0	0
	DUT			0.55	0.5		0.45	1.5			0.55				0.55	-0.95
	Technion			0			0.5	0.5							0	-0.5
	RISOE			1			1	2			1				1	-1
	DTU			1				1			1				1	0
	FFA						1	1							0	-1
	CRES			0			1	1							0	-1
	NTUA	0.25	0.25				1	1.5	0.25	0.25				0.5	1	-0.5
TOTAL		0.25	0.25	2.55			6.95	10.5	0.25	0.25	2.55	0	0	0.5	3.55	-6.95
18. Coordination	ECN	1.5	1.5	1.5	3	1	2	10.5	3.43	2	4.6	1.5	1	1.5	14.03	3.53
(incl. damage of	NLR							0					0.31		0.31	0.31
wind tunnel model)	DUT							0							0	0
	Technion							0							0	0
	RISOE							0							0	0
	DTU							0							0	0
	FFA							0							0	0
	CRES							0							0	0
	NTUA							0							0	0
TOTAL		1.5	1.5	1.5	3	1	2	10.5	3.43	2	4.6	1.5	1.31	1.5	14.34	3.84
	Partner	Planned effort (mm)						Total	Actual effort						Total	Deviation
		Year 1	Year 2	Year 3	Year 4	Year 5	Year 6		Year 1	Year 2	Year 3	Year 4	Year 5	Year 6		
Overall	ECN	8.3	2.5	2.7	3.1	1	11.5	29.1	5.46	5.72	6.4	2	1	3.6	24.18	-4.92
	NLR	6.425	0.375	1	0.2	0	7.7	15.7	3.56	3.04	1.7	0.05	1.03	7.67	17.05	1.35
	DUT	2.29	4.5	4.05	1.75	0	3.2	15.79	3.3	2.25	4.55	2.25	4	0	16.35	0.56
	Technior	1.1	4.9	3.5	0.5	0	5.3	15.3	2.6	6.4	38	0	0	0	47	31.7
	RISOE	5.6	0	4	4	0	9.5	23.1	8	0	2	1.44	0	2	13.44	-9.66
	DTU	2	2	3.5	0.5	0	7	15	2	2.5	9	1	0	2	16.5	1.5
	FFA	1.5	2	0.5	0.5	0	5.3	9.8	2.5	1.9	0.2	0	0	0	4.6	-5.2
	CRES	6.8	0	1	3.75	0	12.75	24.3	10.64	1	1	0	0	9	21.64	-2.66
	NTUA	5.5	2.75	0	0	0	2.25	10.5	5.5	2.25	0	0	0	0.5	8.25	-2.25
TOTAL		39.515	19.025	20.25	14.3	1	64.5	158.59	43.56	25.06	62.85	6.74	6.03	24.77	169.01	10.42